Contents

Editorial
The history of ECMWF 1

News
Changes to the operational forecasting system. 2
New items on the ECMWF web site 2
Workshop on the representation of subgrid processes using stochastic-dynamic models 2
ECMWF Education and Training Programme for 2006. . . 4
ECMWF Forecast Products Users Meeting 5
High-precision gravimetry and ECMWF forcings for ocean tide models. 6
Use of data from the new NOAA-18 satellite 7

Meteorology
Severe Weather Catalogue for the Netherlands and use of ERA-40. 7
New observations in the ECMWF assimilation system:Satellite limb measurements 13
The local and global impact of the recent change in model aerosol climatology 17
Ocean analysis at ECMWF: from real-time ocean initial conditions to historical ocean reanalysis 24

General
ECMWF Calendar 2005/2006 32
ECMWF publications. 32
Index of past newsletter articles. 33
Useful names and telephone numbers within ECMWF . 35

European Centre for Medium-Range Weather Forecasts
Shinfield Park, Reading, Berkshire RG2 9AX, UK
Fax: . . . .+44 118 986 9450
Telephone: National 0118 949 9000
International . . . .+44 118 949 9000
ECMWF Web site . . . . .http://www.ecmwf.int

The ECMWF Newsletter is published quarterly. Its purpose is to make users of ECMWF products, collaborators with ECMWF and the wider meteorological community aware of new developments at ECMWF and the use that can be made of ECMWF products. Most articles are prepared by staff at ECMWF, but articles are also welcome from people working elsewhere, especially those from Member States and Co-operating States. The ECMWF Newsletter is not peer-reviewed.

Editor: Bob Riddaway

Typesetting and Graphics: Rob Hine

Front cover
Image courtesy of the Japanese Argo programme.

Editorial

The history of ECMWF

The ECMWF Convention came into force on 1 November 1975, thus formally establishing the Centre on that date. However the first Director, Aksel Wiin-Nielsen of Denmark, had taken up his duties almost two years earlier, on 1 January 1974. As a result ECMWF is now in its thirties. It is widely acknowledged as a successful European development and recognized as a world leader in the field of numerical weather prediction.

In early 2003, Lars Prahm, then President of the ECMWF Council, proposed to David Burridge, then the Director, that it was time to record the history of the Centre, while those involved are able to contribute their memories. In June 2003, the Council supported the proposal. Austin Woods, who had served as Secretary to the Council since 1984 and retired on 31 December 2004, was commissioned to carry out the work. This took him into the first 18 months of his retirement. Many present and former staff contributed, either by providing input or by reviewing the text. It is interesting to note that the history of ECMWF drew the attention of the scientific publishing house Springer who agreed to publish and distribute it. The result, a book entitled "*Medium-Range Weather Prediction — the European Approach*" authored by Austin, has just been published.

This authoritative and readable book gives an overview of the foundation and establishment of ECMWF. It reviews the work of the Centre during its first three decades and tells the interesting story of how it was conceived in the confusing and difficult political period of the 1960s in Europe. Also the political, scientific, technical and financial discussions that led to its establishment are summarised, as is how ECMWF came to be built 60 km west of London, England. The reader will see how with friendly help the Centre "hit the ground running". The development of ECMWF in the early and formative years and the advances of its science and technology over the following decades are reviewed. The book conveys a sense of what it was like to be a participant during the exciting time at the beginning, and over the years as the Centre matured. In addition the book shows how some major scientific orientations were decided.

As well as describing the development of the analysis and prediction models required for medium-range forecasting, the book covers seasonal prediction, ocean wave forecasting, ensemble prediction, use of satellite data, reanalysis of archive data, development of supercomputers and telecommunications, and commercial issues in meteorology. The book ends with a review of the likely developments in science and technology in the coming years.

I am sure that many readers of the *ECMWF Newsletter* will find the time to read the story of ECMWF. I hope that they will find in the book further reasons to participate in the work of ECMWF or support its future development.

Dominique Marbouty

Changes to the operational forecasting system

Antonio Garcia-Mendez

Changes to the Operational System

There have been no changes to the Operational System since the last issue of the Newsletter.

Planned changes

The e-suite for Cy29r3 has started to cycle for the T799 assimilation and forecasting system. The changes in the Cy29r3 e-suite are as follows.

- Increase in horizontal resolution to T_L799 for the deterministic forecast and the outer loops of 4D-Var.
- Increase in vertical resolution to 91 levels. Model top raised to 0.01 hPa.
- Increase in horizontal resolution to T_L255 for the second inner loop of 4D-Var.
- Increase in horizontal resolution to T_L399 and in vertical resolution to 62 levels (model top ~5 hPa) for the EPS.
- Increase in horizontal resolution to 0.36 degrees for the wave model.
- Use of grid-point humidity and ozone in 4D-Var.
- Revised coefficients (version 2.3) from Météo-France for the linearised ozone chemistry scheme of Cariolle and Déqué.
- Use of Jason altimeter wave height data and ENVISAT ASAR spectra in the wave model data assimilation. ERS-2 SAR spectra are no longer assimilated.

More details (including test data) which will support Member States in preparing for this change can be found at:

www.ecmwf.int/products/changes/high_resolution_2005

New items on the ECMWF web site

Andy Brady

Proceedings of ECMWF Forecast Products Meeting

ECMWF organizes an annual meeting of users of its medium-range and extended-range products. The purpose of the meetings is: to give forecasters the opportunity to:

- Discuss their experience with and to exchange views on the use of the medium-range products, including ensemble products.
- Review the development of the system and discuss future developments.

A report about this meeting is given in the article by Horst Böttger in this edition of the Newsletter. The proceedings are now available from the 2005 meeting.

www.ecmwf.int/newsevents/meetings/forecast_products_user/

Operational Upgrade – 2005 High Resolution Upgrade

The plan to upgrade both the horizontal and vertical resolution of the ECMWF deterministic, Ensemble Prediction (EPS) and monthly forecasting systems is documented here. The upgrades do not apply to the ECMWF seasonal forecasting system. More detailed information is given in the item above about changes to the operational forecasting system.

www.ecmwf.int/products/changes/high_resolution_2005.html

ECMWF Annual Seminar Proceedings – Global Earth System Monitoring

The 2005 ECMWF Annual Seminar was entitled "Global Earth System Monitoring". The presentations and proceedings are now available.

www.ecmwf.int/newsevents/meetings/annual_seminar/2005/

Workshop on the representation of subgrid processes using stochastic-dynamic models

Martin Miller and Tim Palmer

Major causes of error in weather and climate predictions arise from uncertainties about the initial atmospheric state and imperfections in the formulation of the numerical model. Some of the model errors are associated with the parametrization of physical processes. In the context of ensemble prediction, there is a hierarchy of approaches to the representation of this model uncertainty.

- Multi-model ensemble using different models.
- Multi-parametrization ensemble using a number of parametrization schemes with a single model.
- Multi-parameter ensemble where parameters are perturbed within a fixed set of parametrizations in a single model.

In the ECMWF Ensemble Prediction System (EPS) the uncertainty associated with parametrization is represented by introducing a simple stochastic term in the tendencies from the parametrization schemes. It has been found that this approach has a positive impact on the skill of the EPS in the medium range. However, to represent the model

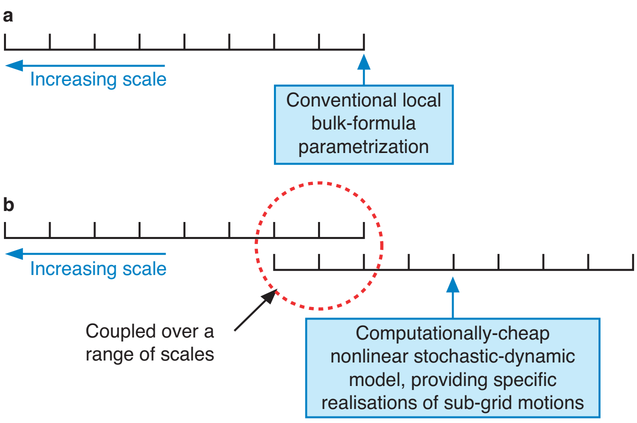

Figure 1 Schematic for (a) conventional weather and climate prediction models and (b) weather and climate prediction models using simplified stochastic-dynamic model representations of unresolved processes.

uncertainty associated with subgrid processes more accurately a more physically based approach is required.

Conventional parametrization schemes use the resolved variables at gridpoints to diagnose the effect of subgrid processes in terms of the mean of an ensemble of sub-grid circulations. However, it is important to take into account the spectrum of fluctuations which occur on the subgrid scale. For example, small changes in boundary layer temperature and humidity can have a significant impact on whether convection occurs. To address this problem stochastic-dynamic systems are being developed to more explicitly represent these fluctuations in parametrization schemes. The difference between the conventional and stochastic-dynamic approaches to parametrization is illustrated by Figure 1.

A workshop on the representation of subgrid processes using stochastic-dynamic models was held at ECMWF from 6 to 8 June. It considered the theoretical developments in this area and the impact of the new stochastic-dynamic subgrid schemes on ensemble forecast skill and model system errors. As part of the workshop three working groups were established. The following summarises the recommendations of the working groups.

Evidence from observation and direct numerical simulation

Field observation programmes and numerical simulations can provide information about the statistical distribution of the parametrized processes. An example is the parallel running of fine- and course-resolution models (i.e. course graining) to get these distributions. However, there is still an issue about how best to implement these results from model experiments and observational analysis into operational models. The working group recommended that:

- With regard to the underprediction of energy in the tail of the energy spectrum of NWP models, tests should be carried out with a spectral backscatter scheme based on EDQNM (eddy-damped quasi-normal Markovian) turbulence theory.
- Consideration should be given to using the coarse-graining strategy to determine the statistics of an effective stochastic parameters function for use in the EPS and seasonal forecasting.
- Consideration should be given to the use of a cloud resolving model (CRM) to provide statistical information concerning the relationship between surface fluxes and coarse-grained model flow states.
- In addition to traditional analyses like spectra and spatio-temporal correlations, a methodology is developed to diagnose the spectral energy transfer, quantify the direction of spectral transfer and acquire insight into the variability of upscale/downscale events.

The parametrization problem in weather and climate models

The study and parametrization of stochastic processes is a promising and rapidly evolving area of research in the atmospheric and oceanic sciences. Several formulations of the general problem are useful at this point, and explorations are proceeding with many models and approaches. Promising avenues include (but are not restricted to) studying differences between high- and low-resolution models, reconsidering numerical and data-assimilation methods in this context, and studying a hierarchy of models and approaches for sub-grid-scale processes. The issues of how to combine stochastic with deterministic representations of weather and climate processes are at the frontier of the field. The working group recommended that:

- ECMWF continues to study the parametrization of stochastic processes in NWP and climate models.
- Tendencies from higher-resolution versions of the ECMWF model are compared with tendencies from lower-resolution versions to provide insights on how to best approximate sub-grid-scale processes.
- A hierarchy of models and approaches are used in research on optimizing the simulation and parametrization of the subgrid-scale processes.
- ECMWF interacts with the academic community in applied mathematics, statistical physics, and the geosciences at large in exploring the issues associated with using stochastic-dynamic models to represent subgrid processes, finding solutions, and implementing the proposed solutions into operational models.

Issues in convection

It is recognised that there are several outstanding problems with current convective schemes in general, and the ECMWF Integrated Forecasting System (IFS) in particular. For example, convection schemes are generally unable to represent the propagation and organisation of convection since they are column based, and the relationship to the large-scale circulation is non-trivial. In addition, convection schemes are inherently "noisy", lack a mechanism for convective initiation to be linked to subgrid fluctuations, and tend to lack sufficient sensitivity to humidity, particularly in mid-troposphere. The working group recommended that:

- ECMWF continues to develop stochastic convective parametrization.
- The new version of the model which allows a separate filter scale for the physics is used to investigate such issues as the

effect of parametrization noise added on scales larger than the grid scale.
- Comparisons are made between ECMWF's approach to stochastic convection and that taken by others.
- The physical basis of the stochastic scheme based on cellular automata is identified and explored.
- There is increased validation of stochastic convective schemes in the context of the EPS, in addition to the deterministic model.
- Improvements are targeted at the statistics of specific physical phenomena, and an attempt is made to identify the pathway by which the stochastic variability influences the relevant validation scores.

Concluding remarks

The annual Research Department workshops are intended to provide input and guidance for its research plans, and this specific one undoubtedly did this. ECMWF was the first modelling centre to introduce stochastic physics into its global model and compared to many previous workshops this one was unusual in discussing a relatively new and developing subject. As such it served not only to help our research but, as importantly, to encourage the wider research community that this topic has 'serious' users in atmosphere and ocean modelling. By the publication time of this article the workshop proceedings should be available.

ECMWF Education and Training Programme for 2006

Umberto Modigliani and Renate Hagedorn

An extensive education and training programme is run by ECMWF to assist Member States and Co-operating States in the training of scientists in numerical weather forecasting, and in making use of the ECMWF computer facilities. The training courses consist of modules that can be attended separately. A student may decide to attend different modules in different years.

Further information about the content of the ECMWF Education and Training Programme for 2006 and the application procedure will be made available at:
http://www.ecmwf.int/newsevents/training/index.html

Computer User Training Course

The objective of the Computer User Training Course is to introduce users of ECMWF's computing and archiving systems to the Centre's facilities, and to explain how to use them. The course is divided into five modules.

COM SMS	16-17 Feb	SMS/XCdp
COM INTRO	20-24 Feb	Introduction for new users/MARS
COM MAG	27-28 Feb	MAGICS
COM MV	1-3 Mar	METVIEW
COM HPCF	6-10 Mar	Use of supercomputing resources

Each module will consist of some lectures and some practical sessions. All the lectures will be given in English. A workbook will be provided for each module, together with basic manuals and other relevant documentation. A set of lecture notes are available at:
www.ecmwf.int/services/computing/training/material/
Students attending any part of the course should:
- Have experience of a computer system elsewhere.
- Be familiar with ANSI Fortran 77 or 90.
- Know basic UNIX commands.
- Be able to use an editor (e.g. *vi*).

Meteorological Training Course

The objective of the Meteorological Training Course is to provide advanced training in the field of numerical weather forecasting. The course is divided into five modules. The MET OP module is designed to cover operational aspects of weather forecasting, whereas the other modules are more geared towards research aspects of numerical weather prediction.

MET OP-I	13-17 Mar	Use and interpretation of ECMWF products
MET DA	22-31 Mar	Data assimilation and use of satellite data
MET PR	24-28 Apr	Predictability, diagnostics and seasonal forecasting
MET PA	2-12 May	Parametrization of diabatic processes
MET NM	15-24 May	Numerical methods and adiabatic formulation of models
MET OP-II	5-9 Jun	Use and interpretation of ECMWF products

All the lectures will be given in English. A set of lecture notes are available at:
www.ecmwf.int/newsevents/training/lecture_notes/
Students attending the course should:
- Have a good meteorological and mathematical background.
- Be familiar with the contents of standard meteorological and mathematical textbooks.

Annual Seminar and Workshops

In addition to the training courses, there will be an Annual Seminar. This consists of a one week series of lectures by both ECMWF and invited experts to discuss progress in a selected topic related to numerical weather forecasting. There will also be a number of workshops covering various operational and research activities. Information about these events will be available later in the year.

ECMWF Forecast Products Users Meeting

Horst Böttger

The ECMWF Forecast Products Users Meeting was held at the Centre's headquarters in Reading from 15 to 17 June 2005. The annual event was well attended with participants from most of our Member States and Co-operating States. In addition there were representatives from two private sector service providers as well as some end users of our products.

During the three-day meeting we addressed issues related to the full range of ECMWF products, form the medium-range via the monthly to the seasonal forecast range. On the first day ECMWF staff provided information on the status, development and performance of the operational forecasting suite, addressing in particular the changes which are planned for implementation over the coming twelve months. On the other two days users gave presentations on applications of medium- and extended-range forecasts followed by several presentations by participants from our Member States and Co-operating States about the use and evaluation of ECMWF products on all time ranges. The meeting concluded with a plenary session during which some conclusions and recommendations were formulated. This article provides a brief summary of the salient points from the discussions and conclusions.

The performance of the forecasting system over the previous twelve months was summarised based on the evidence from ECMWF and the Member States. The excellent performance of the deterministic medium-range forecasting system was acknowledged. During winter 2004/5 the results in the free atmosphere over the northern hemisphere had been outstanding. Over Europe a consistent upward trend in skill was reflected in the 500 hPa height anomaly correlation scores. It was also noted that recent changes in the forecasting system had a positive impact on the performance of the Ensemble Prediction System (EPS).

The long-term trend in skill of precipitation forecasts was reviewed in some detail. A one-day gain per decade in predictive skill was demonstrated for moderate amounts of precipitation. However, such levels of skill could not be found for large amounts. Results got more robust when verifying forecasts against up-scaled precipitation analyses based on observations from high-density observation networks. Member States were encouraged to continue with the timely provision of precipitation observations from high-density national networks. Problems had occurred with the treatment of low-level clouds during persistent inversions over central Europe in winter. Users were informed that the improved boundary layer cloud system, which was introduced in April 2005, will help alleviate these deficiencies.

There was appreciation of the availability of severe weather products via dissemination and the web. Both the tropical cyclone tracks and derived strike probabilities, and the Extreme Forecast Index (EFI) are based on the EPS and reflect a probabilistic approach towards the prediction of severe weather events.

The monthly forecasting system had been operational since October 2004. Product dissemination was added in spring 2005. There was still some lack of experience with these products in Member States. ROC area scores from ECMWF indicated some skill over persistence in the predictions of two-metre temperature anomalies for days 12-18, but to a lesser extent for days 19-32. Good predictions of transitions between flow regimes last winter were acknowledged. The seasonal forecasting system had been particularly successful in predicting consistently the dry conditions over the Iberian Peninsula since November 2004. Potential benefit was expected from the multi-model system. A reduced RMS error and improved correlation was demonstrated for NINO3 sea surface temperature forecasts.

The planned developments of the forecasting system were described, with particular emphasis on two key changes.

- ◆ Upgrades to the horizontal and vertical resolutions of the forecasting system (T_L799L91 for the deterministic system and T_L399L62 for the EPS).
- ◆ Implementation of the unified system (VAREPS) with an extension of the medium-range forecasts to 15 days. Running the EPS to 15 days at the planned resolution of T_L399 will not be affordable. The VAREPS configuration is based on a reduction in resolution on day 7 to T_L255. VAREPS is expected to be merged with the monthly forecasts at a later stage.

The planned establishment of a web information system about operational changes was welcomed. This system has now been implemented at:

www.ecmwf.int/products/changes/high_resolution_2005.html

It provides details of the planned changes, target dates, and information about available test data sets. A range of new products, such as EPSgrams, will be developed for the extended-forecast range to 15 days and for the unified forecast system. There are requirements for global and regional EFI products, and new monthly forecast products for which verification should be added. Initially, new products will be made available on the web for assessment by Member States and Co-operating States.

The presentations by participants from Member States and Co-operating States described a wide range of applications and usage of medium- and extended-range products. Several countries now provide probabilistic forecast information to the public through the web, in newspapers and on television. Also some traders in the energy market complement the deterministic outlook with probabilistic information to create a level of confidence in the forecast. The experimental use of probabilistic information from the medium- and extended-range ensemble forecast systems was reported by several countries. In Member States the development of limited area ensemble prediction systems is an increasing area of research and development. A few such systems have been transferred into operations - examples are COSMO-LEPS (Consortium for Small-scale Modelling-Limited Area-Ensemble Prediction System, members are Germany, Greece, Italy and Switzerland) and LAMEPS (Limited Area Model EPS run by Norway).

A list of new user requirements was drawn up based on requests expressed during the meeting. Most of these requirements were for more products to be made available either through enhancements in the model post-processing or through development work to be undertaken by ECMWF. Users supported the Centre's plans to develop products for the extended medium-range to 15 days and from the unified system. There were also some specific requests.

- Global EFI products to be made available to WMO members.
- Hindcast periods and reference periods for anomalies to be standardized, in particular when developing combined and calibrated multi-model products, due to the increasing importance of providing hindcast data for product calibration.
- ECMWF to provide support for time critical applications which are run at the Centre by Member States, noting that a framework for such activities had been developed and will be released later this year.

User also stressed the importance of timely forecast delivery. The introduction of the Early Delivery System in 2004 had resulted in a significant improvement in the operational usefulness of ECMWF products. A recommendation was formulated to review the delivery times of products after the implementation of the planned upgrades of the forecasting system later in 2005 and early 2006.

The programme of the meeting together with the presentations and the conclusions from the final discussion can be found on the web at:

www.ecmwf.int/newsevents/meetings/forecast_products_user/presentations.html

High-precision gravimetry and ECMWF forcings for ocean tide models

Anthony Hollingsworth

Atmospheric analyses produced by ECMWF are used in many areas in Earth Science, and in the interpretation of remotely sensed data. Familiar examples include the use of the following.

- ECMWF operational and reanalysed wind stresses and surface fluxes of heat and moisture to force ocean models.
- ECMWF temperature and humidity fields to calculate the "dry" and "wet" effects on radar altimetry from space.

An interesting new example is the exploitation of the tides in the ECMWF surface pressure analyses for the interpretation of gravimetric measurements from space. NASA's high-precision gravimetry mission, GRACE (www.csr.utexas.edu/grace/) is aimed at studying temporal changes in the Earth's gravity field, such as variations due to seasonal changes in soil moisture. A study by *Andersen et al.* (2005) shows remarkable comparisons of inter-annual changes in European summer soil moisture estimated from the GRACE gravimetry mission, and by the operational ECMWF soil-moisture analysis. Success in exploiting GRACE data requires extraordinary precision in calculating tidal effects in the ocean, and then removing those effects from the GRACE measurements.

The launch of NASA's GRACE gravimetry mission raised new demands on the accuracy of models of ocean tides, and thus on the accuracy of atmospheric tides in the ECMWF analyses used to force such models. The success of the ECMWF analyses in meeting the demands has been assessed in the studies carried out by *Ponte & Dorandeu* (2003) and *Ray & Ponte* (2003). Besides the prominent S2 and S1 (solar semi-diurnal and diurnal) atmospheric tides, these investigations detected weak atmospheric tides such as the M2 (lunar semi-diurnal) tide and the P1 and K1 declinational tides, an impressive result.

Another impressive result in this series of studies is a successful simulation of the global S1 ocean tide by *Ray & Egbert* (2004). The small S1 ocean tide is forced primarily by diurnal atmospheric pressure loading. The ocean-tide S1 simulation was forced by the S1 atmospheric pressure tide extracted from the ECMWF analyses, and was successfully verified against Topex/Poseidon radar altimeter data, and against tide-gauge data.

One of the difficulties affecting the use of ECMWF analyses for work of this kind is the need for a good time interpolation of the semi-diurnal S2 tide, when using six-hourly archived data. A recent investigation by *Dobslaw & Thomas* (2005) uses ECMWF three-hour forecasts to address the time-interpolation problem. They go so far as to suggest that "[ECMWF] forecasts allow one to account for atmospheric variability and corresponding oceanic responses down to semidiurnal timescales, dispensing with any additional model of atmospheric tides".

A general result noted by all these authors is the benefit for ocean-tide (and thus gravimetry) studies of having in the ECMWF pressure analyses a faithful representation of substantial seasonal and other low-frequency variations in the atmospheric tides.

Accurate modelling and assimilation of the diurnal cycle has been a constant concern at ECMWF since the early 1980s, because of the need to avoid aliasing of diurnal phenomena into synoptic phenomena. A general review of tides in the analyses is provided by *Hsu & Hoskins* (1989). Some of the reasons for the success of the atmospheric analyses of the dominant S2 tide are discussed by *Janssen* (1999). He concluded that because stratopause temperatures are as they are, the tides in the model are surprisingly insensitive to the model's treatment of the upper boundary condition. If stratopause temperatures were 20 K warmer, the atmosphere would be much closer to resonance and so the model would have much more difficulty in simulating the S2 tide. In this sense we and the oceanographers are lucky. Janssen's results also explain the reasons for small phase errors in the model's air tides.

We have already noted the use of GRACE data to validate ECMWF's soil-moisture analyses. Looking to the future, gravimetric data from GRACE and from ESA's GOCE mission (www.esa.int/esaLP/ESAYEK1VMOC_goce_0.html) will be used to define the Earth's geoid with unprecedented accuracy, thus providing a much improved understanding of ocean currents, and so providing another benefit for ECMWF's seasonal forecast activity.

FURTHER READING

Andersen, O.B., S.I. Seneviratne, J. Hinderer and **P. Viterbo**, 2005: GRACE-derived terrestrial water storage depletion associated with the 2003 European heat wave. *Geophys. Res. Lett.*, **32**, doi:10.1029/2005GL023574 (to appear).

Ponte, R.M. and **J. Dorandeu**, 2003: Uncertainties in ECMWF surface pressure fields over the ocean in relation to sea level analysis and modelling. *J. Atmos. Oceanic Technol.*, **20**, 301–307.

Ray, R.D. and **R.M. Ponte**, 2003: Barometric tides from ECMWF operational analyses, *Annales Geophysicae*, **21**, 1897–1910.

Ray, R.D. and **G.D. Egbert**, 2004: The global S1 tide. *J. Physical Oceanography*, **34**, 1922–1935.

Dobslaw, H. and **M. Thomas**, 2005: Atmospheric induced oceanic tides from ECMWF forecasts. *Geophys. Res. Lett.*, **32**, L10615, doi:10.1029/2005GL022990.

Hsu, H-H. and **B.J. Hoskins**, 1989: Tidal fluctuations as seen in ECMWF data. *Q. J. R. Meteorol . Soc.*, **115**, 247–264.

Janssen, P.A.E.M., 1999: On tides in the ECMWF model. *ECMWF Tech. Memo. 284* (downloadable from www.ecmwf.int/publications/library/do/references/list/14).

Use of data from the new NOAA-18 satellite

Anthony McNally

The NOAA-18 (N) spacecraft lifted off on 21 May 2005 from Vandenberg Air Force Base, California, on a Boeing Delta II expendable launch vehicle. The first data from the NOAA-18 spacecraft was received at ECMWF on 4 July and one week later we began operational monitoring of the radiance observations from the HIRS (High-resolution IR sounder), AMSUA (Advance Microwave Sounding Unit) and MHS (Microwave Humidity Sounder) instruments. Having established the quality and stability of the data (and tuned the various bias correction parameters needed by the assimilation system), radiances from the AMSUA instrument were introduced in to ECMWF operations on 8 September. Active use of the HIRS and MHS instrument will follow in the near future as our monitoring has confirmed that the data quality is very good. This is particularly significant for the latter as the MHS is a completely new instrument procured by EUMETSAT primarily to serve on the METOP polar platform due for launch in 2006. Apart from giving confidence in the instrument design, data from the NOAA-18 MHS will be used to test the METOP ground segment with real observations prior to the launch of METOP.

Severe Weather Catalogue for the Netherlands and use of ERA-40

Geert Groen and Robert Mureau
KNMI, The Netherlands

At KNMI there is a long meteorological tradition not only in investigating, observing and forecasting the weather, but also in providing warnings of severe weather. Its founder Prof. C.H.D. Buys Ballot (in 1854) introduced, for instance, wind warnings for shipping. Soon the surge warnings for the Dutch coast followed. Over the last century warnings for fog, slippery roads, thunderstorms and other specialised warnings were introduced.

At the end of the 20th century the provision of severe weather warnings got a real boost. KNMI was given by law the authority to coordinate the warnings for major disruptive weather events, and severe weather warnings became part of its core business. In 1999 an extensive system for alarms and (early) warnings was implemented. In cases of severe, disruptive weather KNMI issues a so-called weather-alarm for the Netherlands via teletext, internet and broadcasters. For less severe weather regular warnings have been designed for special user groups (aviation, shipping, traffic etc.).

A system like this needs evaluation and verification. All events and warnings have been evaluated since 1999 not only for verification but also to increase operational knowledge. However, severe weather occurs on average about 5–10 times per year. The definition of an alarm is made bearing in mind that (a) we do not want to issue warnings too often and (b) it could be argued that extreme weather that occurs more than 10 times per year will not be considered disruptive because society will be better prepared. Clearly there was a sampling problem. Six years of weather alarm resulted in about 50-60 cases. About half of them were thunderstorms,

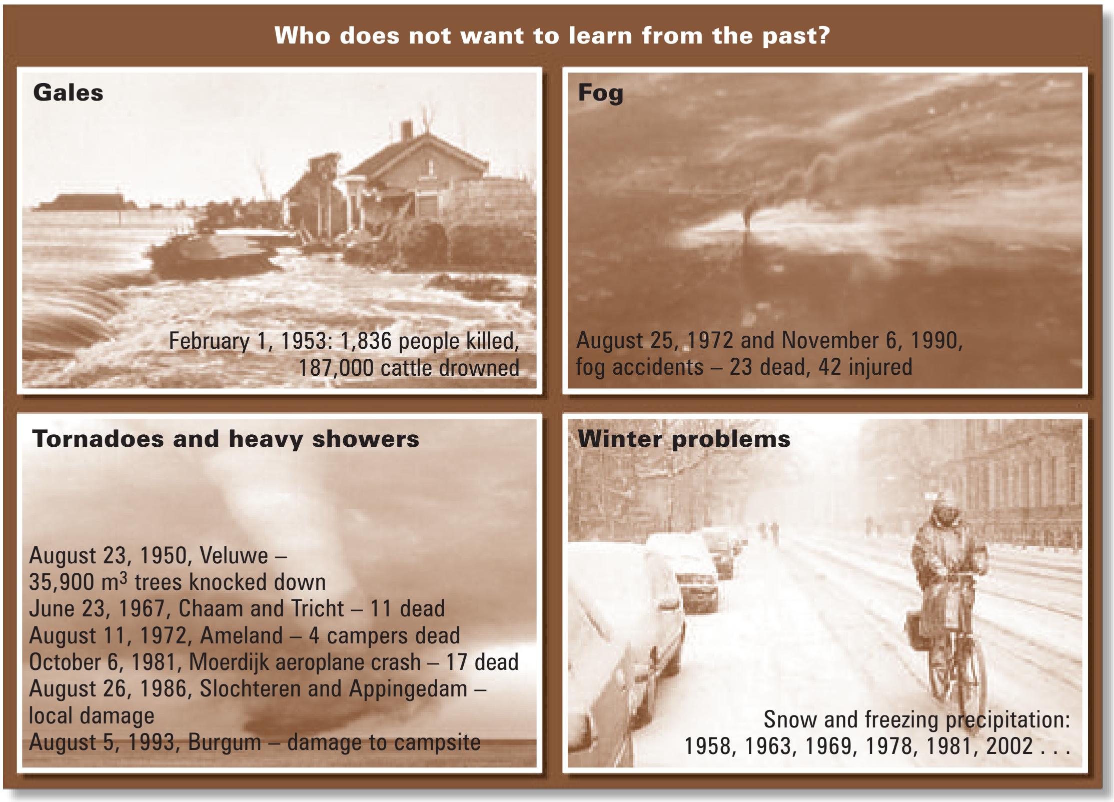

Figure 1 Examples of dates and features for the Catalogue on Severe Weather.

the rest a variety of other events. We only have a very chaotic data set: there are many lists of events, damage reports, station observations, hand drawn maps, case studies and newspaper articles. Some examples of severe weather events affecting the Netherlands are given in Figure 1. All very interesting but not very useful for the evaluation of a modern warning system. But why not use the ERA-40 data produced at ECMWF?

The reanalysis project ERA-40 covers the period from September 1957 to August 2002. Three-dimensional variational techniques are applied using the T159L60 version of the Integrated Forecasting System (IFS) to produce the analyses. These involve comprehensive use of satellite data, starting in 1972, with Atmospheric Motion Vectors (AMVs) used from 1979 onwards. ERA-40 provides analyses for every six hours throughout the period, supplemented by forecasts. The products are of a reasonably high temporal and spatial resolution, with a grid-spacing close to 125 km in the horizontal and with sixty levels in the vertical.

ERA-40 and historic events

So far, ERA-40 has been used mainly for climatological studies (e.g. statistics and trends). But some studies have made use of "extreme" information from the archives. In 1953 a severe storm caused a devastating flood in the Netherlands and surrounding countries resulting in almost 2,000 casualties and more than 187,000 cattle deaths. The meteorological situation was reanalysed fifty years later, in 2003, with data from ECMWF, NCEP, HIRLAM and WAQUA (the Dutch wind surge model). The reanalyses gave an excellent reproduction of the synoptic situation and it was also demonstrated that a modern forecast would have given one extra day for taking precautionary measures. Something similar was shown in a study by *Jung et al.* (2003) for the Hamburg storm on 17 February 1962. This storm was well predicted by single deterministic forecasts 84 hours in advance.

This inspired us to start looking, in a more systematic way, in the ERA-40 database. We restricted ourselves to about five cases of severe weather per year, concentrating on the Netherlands, and using observations and impact reports as the search key. Our initial goal was to "collect" events in a series of reanalyses, with a five-day lead time with respect to the event. The fields retrieved are mean sea level pressure, winds at 300 and 500 hPa, wet bulb potential temperature (θ_w) at 850 hPa, potential vorticity etc.

It is recognised that the resolution (space and time) of ERA-40 is relatively coarse compared with operational high-resolution data assimilation systems. We can only hope to capture most of the large-scale dynamical conditions, even when the synoptic events occur on a smaller scale in time and space.

The synoptic reconstruction consists of a combination of ERA-40 model data and historic weather charts, surface and upper-air observations, vertical profiles (if available) and other available background material.

Content of the Catalogue

Currently we have identified 200 cases of severe weather, all relevant for the Netherlands. However, the number of cases will probably rise to more than 300 in the future as these cases are just the result of the first scan. The next step will

Year	Date	Charts	Phenomenon
1953	01 February 1953	28 January–04 February 1953	Extreme flooding
1958	05 January 1958	02–12 January 1958	Very rough week
1958	25 February 1958	22–26 February 1958	Snowstorm (with freezing rain)
1959	7 December 1959	03–09 December 1959	Hurricane on the Atlantic
1960	03 December 1960	29 November–05 December 1960	Storm and extreme precipitation
1962	12 February 1962	09–13 February 1962	Heavy Storm (also inland)
1967	25 June 1967	21–26 June 1967	Tornadoes Chaam and Tricht
1967	17 October 1967	13–17 October 1967	Heavy gale in autumn
1972	25 August 1972	23–25 August 1972	Traffic accident in fog
1976	27 January 1976	22–28 January 1976	Extreme cold period
1983	12 May 1983	06–13 May 1983	Ascension Day storm
1987	17 July 1987	13–18 July 1987	Tornado Oldebroek
1990	25 January 1990	19–26 January 1990	Violent storm

Figure 2 Example of a listing of a subset of the Catalogue. Note that the ERA-40 period is from September 1957 to August 2002; the extreme flooding event of February 1953 has only been analysed as a case study.

be an objective scan of observations under weather alarm criteria. Then we will need to address issues raised by users of the Catalogue.

The Catalogue will be made available on the web. The index provides links to a database containing several severe weather events per year, indicating the dates, type of phenomenon and timescale of each severe weather event. Clicking on the date of the event leads to a short synoptic description of the case. Maps will be available for 5 days ahead of the event (sometimes up to a week), showing the origin of the event, for several appropriate parameters and levels. Several animations will be made available. And there will be a link to the observations and warnings, historic material and background (case study) articles. Initially we will concentrate on the analyses. Later, hindcasts will be added as well. An example of the index of (a subset of) the Catalogue is shown in Figure 2.

What can we learn from the Catalogue?

The catalogue can be used for several purposes apart from testing the severe weather warning system: performing case studies, training of forecasters, building a weather simulator, testing models and e-learning.

- The average forecaster will experience a severe event perhaps once every five years. Using case studies for individual training will allow forecasters to enhance their knowledge of severe weather.
- Developing a weather simulator has been suggested for some years now as training tool for forecasters, but such a simulator has not yet materialized. Creating a meteorological basis for such a simulator with the ability to realistically replay interesting weather events would be a good spin off from this project. The Catalogue offers a variety of observations, model data, background material in one database for many cases, making a simulator a very real possibility.
- The Catalogue will give suggestions for dates for model tests.
- All learning elements can be combined into an e-learning module. The educational training department of KNMI is implementing e-learning in the training of forecasters and special users. Implementation is based on the international experience that e-learning is not just scanning a book to the Web, but creating challenging, interactive lessons. The learning procedure will be a mix of an introduction to a case, followed by a challenge to understand and assess the situation, make decisions before proceeding to the next time-step, and follow the correct procedures. Finally there is a testing of knowledge. This idea has recently been implemented in a training session for maritime users and will be tested this autumn. The Catalogue contains useful information for the e-learning tool. It will provide meteorological material about the evolution of an event as well as background material such as impact-articles.

First impressions

We have started by collecting the storm cases. The first results, confirming the 1953 experiences, were very impressive. The dataset is continuous and of high quality. One of us, being an operational forecaster (GG), was surprised and impressed when comparing historic weather charts to ERA-40 reanalyses of surface pressure and θ_w. The respect goes both ways: the reanalyses look very real (a compliment to modern technology), but the quality of the old "hand" maps makes you aware of the expertise of the operational colleague's over the past 50 years who were able to create maps with very little data. This experience strengthens the (subjective) trust in investigating model data in the reconstruction.

Some disadvantages, experienced so far, are also worth mentioning. The coarse resolution with a grid spacing of 125 km and six-hour intervals limits the detailed study of small-scale storms. A famous storm in the Netherlands (the Ascension Day storm in 1983) originated in the English Channel, developed very quickly and caused havoc in the

ECMWF Analysis Saturday 10 February 1962 12 UTC – Mean Sea Level Pressure

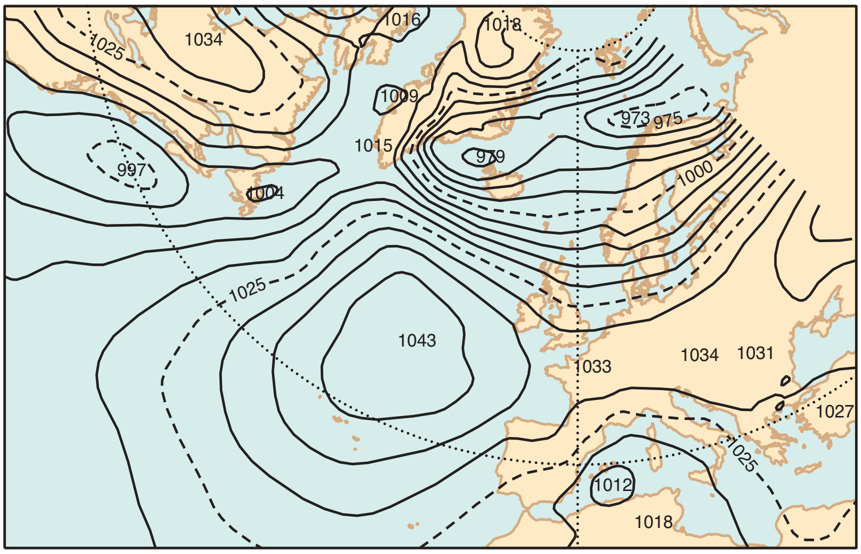

Figure 3 Surface pressure at 12 UTC on 10 February 1962 from ERA-40. Note the steering high over the Atlantic, the low pressure area passes New Foundland.

IJsselmeer. This was captured in a broad sense, but for rapidly developing storms a shorter time step is needed. This will obviously become even more of a problem for cases where the development is mainly driven by convective processes. Nevertheless preliminary results show at least a synoptic signal associated with these smaller severe events. Furthermore we find that, due to the resolution of the surface wind fields, the ERA-40 wind are consistently underestimated with respect to the observations, sometimes up to 3 Beaufort Force. For convective events some extra parameters (e.g. CAPE) would be useful, but they are not part of the current system. The potential vorticity was an incredible asset. It is exciting to study the weather of the 1950s and 1960s through modern "PV-glasses". Looking for instance at a development by means of a loop of potential vorticity is like searching for dry intrusion in loops of water vapour images. From recent knowledge we know that dry intrusion increases rotation or vorticity and stimulates (potential) instability.

Future plans and wishes

There is the obvious wish for higher-resolution analyses. ERA-40 is extremely useful for the general picture and for the large-scale background flow. But when it comes to studying small-scale, rapidly-developing storms more detail in space and time (at least 3-hour analysis steps) is needed. For convective systems even more detail is required in combination with indices such as CAPE.

With the 22 km HIRLAM model we will prepare reanalyses for some selected cases. This might also be taken up by a future ERA project, probably providing higher-resolution reanalyses for the Atlantic-Europe area over the entire period of ERA-40 (i.e. since 1957).

For detailed studies of events there is a need for vertical cross-sections of several parameters (e.g. to compare with the observed radiosonde soundings). This wish requires some form of model-level output, which costs a lot of resources.

Last but not least we would like to promote international cooperation for developing a web-based European Severe Weather Catalogue. Storms do not stop at our borders, and one mesoscale convective situations sometimes hits several countries.

Example of a synoptic reconstruction: The severe storm of 12 February 1962

On 10 February 1962 a series of low pressure areas extends around an extensive area of high pressure with a maximum of 1043 hPa near the Azores. The low causing the storm two days later, is at this time situated near Newfoundland. The centre has a pressure of 1004 hPa (Figure 3) and is moving northeast near the warm side of a jet stream, deepening 14 hPa in 12 hours time whilst moving to Southern Greenland.

As time progresses the track of the low bends from an easterly to an east-southeasterly direction after passing Iceland on 11 February. One day later the pressure has dropped to 972 hPa over the Norwegian Sea and 955 hPa over Southern Sweden. The lowest surface pressure of 950 hPa occurs at around 00 UTC on 13 February 1962 over the Baltic Sea. The broad frontal system of this storm passes the Netherlands on 12 February (Figure 4): the warm front at around 00 UTC on 12 February the cold front almost 24 hours later. The model reanalysis at 12 UTC (Figure 4(b)) can be compared to the historic weather chart (Figure 5). Both the quality of the historic frontal analysis as well as the model reanalysis is shown in the thermal pattern at 850 hPa. The fronts are situated along θ_w values 7–8°C and the occluded part trough the centre of the lower values.

Warnings were issued for Beaufort Force 10 during a period of 24 hours, starting in the evening of 11 February. For a period of six hours a wind of Force 11 was expected along the northern coast. This did not quite materialize. The observed maximum mean hourly wind speed reached Force 9–10 (22 to 25 ms^{-1}); this occurred inland in the Netherlands, rather than at the coast, in the early of the afternoon soon after 12 UTC (13 local time). Note that in the reanalysis near-surface wind speeds reached hourly values (Figure 6) of only Force 6 to 8.

In a winter month like February with most friction over the colder land one should expect the highest wind speeds over

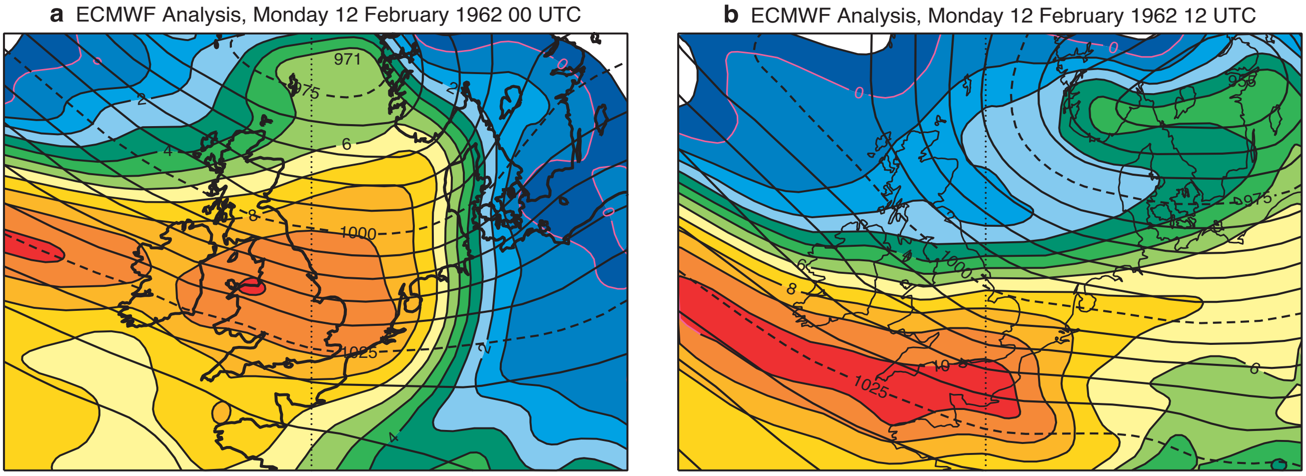

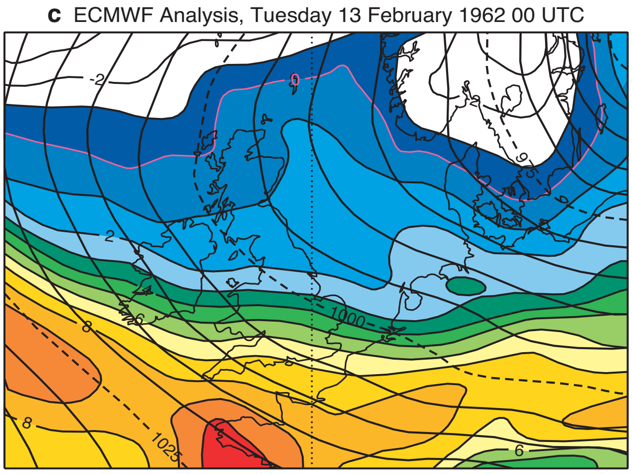

Mean Sea Level Pressure and θ_W at 850 hPa

θ_W (°C)

–1 – 0	2 – 3	5 – 6	8 – 9
0 – 1	3 – 4	6 – 7	9 – 10
1 – 2	4 – 5	7 – 8	>10

Figure 4 Surface pressure and thermal pattern (theta-w) 850 hPa from ERA-40. (a) 00 UTC on 12 February 1962: the low, still deepening, moves to Norway, with the Netherlands and England/Wales in the warm sector. (b) 12 UTC on 12 February 1962: in the warm sector west-southwest winds at 1.5 km height increase to 35–40 ms^{-1}. (c) 00 UTC on 13 February 1962: the storm passes the Baltic Sea with the waving cold front (situated along the 7°C isopleth of θ_w) moving southeast.

the sea and by the coast rather than inland. One explanation for the strong surface winds inland can be found by considering the vertical structure. When the lower profile is unstable, winds aloft in the lower part of the stratosphere, say up to 1.5 km, are strong and vertical exchange of momentum contributes to surface wind speed. In this event the temperature rises in the warm sector from 4 to 10°C and at 1.5 km height wind speeds increase to about 35 ms^{-1}.

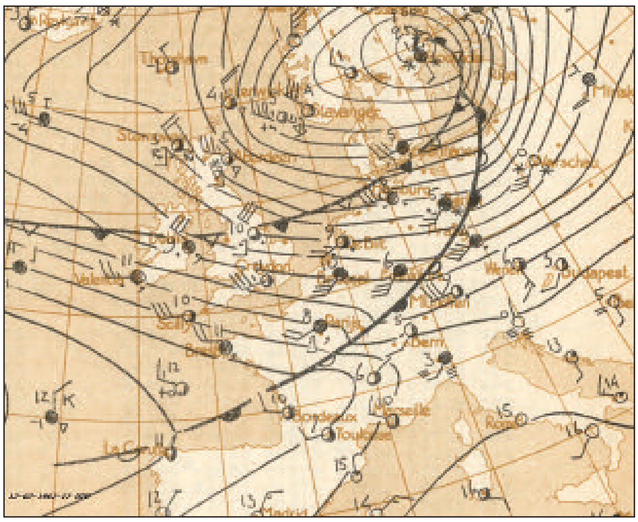

Figure 5 Handrawn surface analysis at 12 UTC on 12 February 1962.

The vertical distribution of temperature, humidity and wind is important for judging stability and advection. Radiosonde soundings contain this historic information. The soundings from De Bilt (central part of the Netherlands)

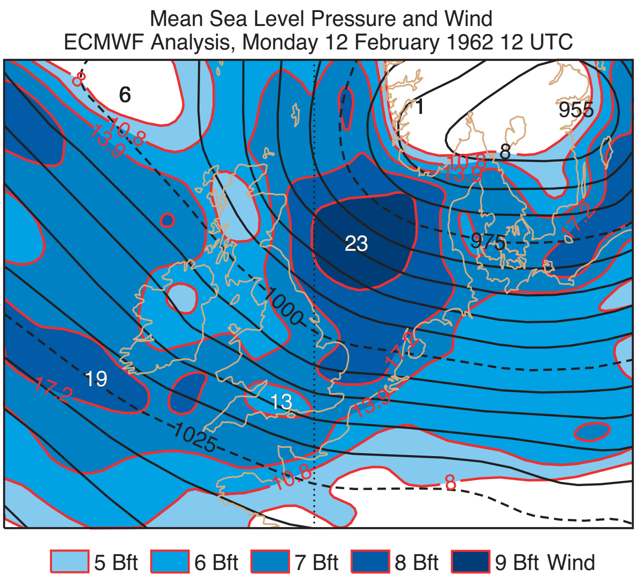

Figure 6 Surface pressure and isotachs at 12 UTC on 12 February 1962 from ERA-40. Note that the wind speed is Force 6 on land and Force 8 near coast; these values are 2 to 3 Beaufort Force too low.

show a weak inversion just above 1 km (Figure 7). In the boundary layer below this inversion the profile is dry adiabatically unstable, giving maximum vertical exchange of momentum. Average hourly wind speeds reach up to 70% of the winds in the free atmosphere at 1 km height and it is likely that maximum gusts reach values close to 90%.

At 12 UTC, in the warm sector, with the cold front just north of the Frisian Isles, the sounding shows some decrease of humidity at 6 km to 75%, a possibly indication of dry air in the higher troposphere. Does this dry intrusion in any way influence the increase of wind speed, for instance by increasing (potential) instability ahead of the surface cold front (split-level cold front)? In the ERA-40's potential vorticity field at 12 UTC on 12 February (Figure 8) this intrusion is obvious over Southeast Scandinavia, thus giving an impulse to the low and increasing (potential) instability on the cold front. Whether this is the case over the Netherlands should be investigated in the future using cross-sections, model soundings and a high-resolution model

The study of this event ends as the cold front passes the Netherlands during the night of 12/13 February, and some waves weaken the frontal speed. After a short break in the wind speed a trough passes in the unstable northwesterly advection of semi-arctic air mass. As sea temperatures are relatively high compared to the colder advection, showers pass the Netherlands with a typical variety of precipitation types such as rain, snow and hail, and sometimes there is a thunderstorm with temperatures dropping to near 0°C.

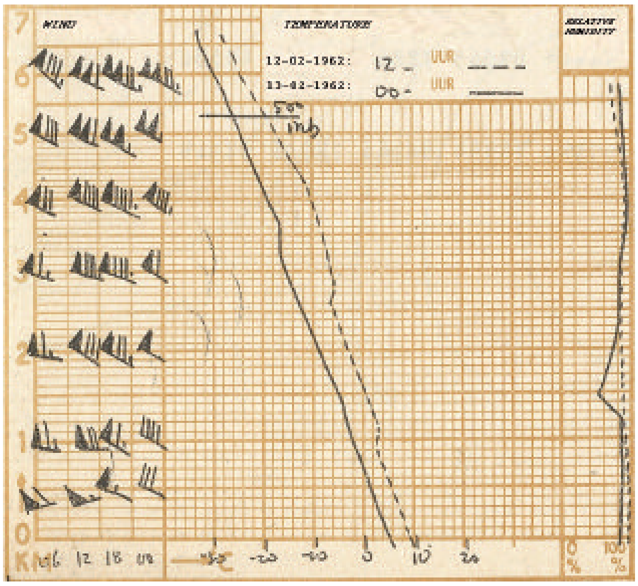

Figure 7 Soundings of temperature (centre), wind (left), relative humidity (right), at 12 UTC (dashed line) and 24 UTC (closed line) on 12 February 1962 at De Bilt. There is a weak inversion at 12 UTC at 1 km height, strong winds and high humidity. At midnight temperature and winds decrease, and the instability increases below 3.5 km. The freezing level sinks from 1.5 km to 700 metres in 12 hours.

FURTHER READING

Newsletter article

This article and all chart animations can be found at:
www.nvbm.nl/Newsletter/Article

Presentation at the ECMWF Forecast Products Users Meeting – June 2005

www.ecmwf.int/newsevents/meetings/forecast_products_user/Groen.ppt

General information on ERA-40

www.ecmwf.int/research/era

The ERA-40 archive

www.ecmwf.int/publications/library/ecpublications/_pdf/era40/ERA40_PRS17.pdf

ECMWF newsletter spring/autumn 2004 about ERA-40

www.ecmwf.int/publications/newsletters/pdf/101.pdf

Investigation of three major European Storms using ECMWF forecast system (*Jung, Klinker and Uppala*)

www.ecmwf.int/publications/library/ecpublications/_pdf/era40/ERA40_PRS_10.pdf

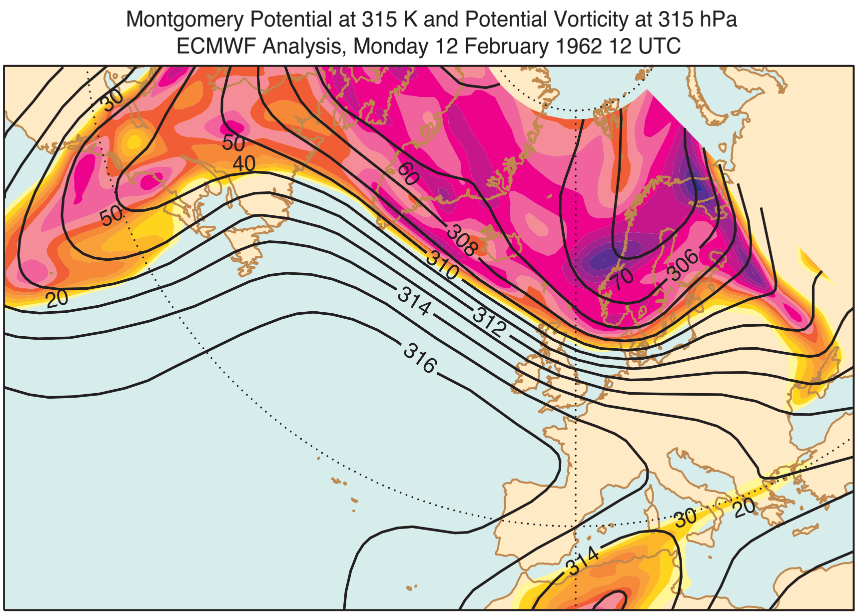

Figure 8 Potential vorticity distribution and the Montgomery Potential at the 315 K surface at 12 UTC on 12 February 1962 from ERA-40. It shows the dynamical tropopause and also how dry stratospheric air overruns the cold front near Denmark.

New observations in the ECMWF assimilation system: Satellite limb measurements

Niels Bormann and Sean B. Healy

A new type of satellite data can now be assimilated at ECMWF: data from limb-sounding satellites. So far, only satellite data from Earth-looking nadir instruments have been used in the ECMWF system. In contrast, the new limb-sounding observations measure atmospheric properties along a line sideways through the atmosphere.

The limb-viewing geometry is well suited to give important information on the vertical structure of the atmosphere and to significantly improve ECMWF's analyses of the tropopause and stratospheric region. Weighting functions in the vertical are much sharper than usually encountered for nadir sounders, as most information typically stems from a shallow layer around the tangent point of the line-of-sight. Two types of limb sounding observations can now be assimilated:

- Bending angle profiles from global positioning system (GPS) radio occultation (RO).
- Emitted clear-sky limb radiances.

Experiments have been carried out at ECMWF using both types of limb measurements. So far the results have been very promising. The RO data leads to clear improvements in terms of stratospheric temperature biases, especially over Antarctica, whereas the limb radiances introduce considerable changes to mean analyses of temperature, humidity, and ozone in the stratosphere. Further research is required regarding the two-dimensional nature of the data. It is expected that eventually limb measurements will be routinely assimilated at ECMWF.

Limb sounding techniques

The GPS RO technique is based on very simple physics — Snell's law of refraction. The basic measurement geometry is illustrated in Figure 1. A radio signal is transmitted by a GPS satellite and measured with a receiver placed on a low earth orbit (LEO) satellite. The ray-path between the satellites is bent as a result of refractive-index gradients in the atmosphere, which in turn are related to gradients in temperature and humidity. The ray-bending angle, α, can be derived from the time required for the radio signal to propagate between the GPS and LEO satellites, and the motion of the LEO satellite enables the variation of α as a function of tangent height to be determined. The GPS RO concept has now been successfully demonstrated with the GPS/MET and CHAMP "proof of principle" missions, and from 2006 the GRAS instrument on METOP and the constellation of six satellites, COSMIC, will provide GPS RO measurements operationally.

The RO data provide high-accuracy information on temperature throughout the upper troposphere and the lower stratosphere, and limited moisture information in the

Niels Bormann is supported by the EU FP5 ASSET Project.

Sean Healy is supported by the EUMETSAT Fellowship Programme.

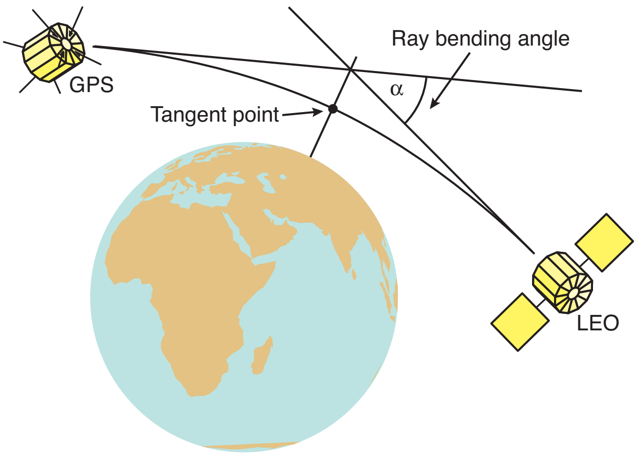

Figure 1 The geometry of a GPS RO measurement. A radio signal is emitted by the GPS satellite and measured with a receiver placed on the LEO. The path of the radio signal is bent as a result of refractive-index gradients in the atmosphere. The motion of the LEO satellite enables the variation of ray-bending with tangent height to be investigated.

upper troposphere. Good vertical resolution, global coverage and all-weather sounding capabilities make GPS RO data an extremely valuable new source of information. In contrast to other satellite observations, in principle GPS RO data should not require a bias correction. This is because, fundamentally, the observation is based on the precise measurement of a time-delay of the GPS signal along the ray-path. Furthermore, the forward modelling is relatively simple, and it is not reliant on spectroscopic parameters or the assumed concentrations of well-mixed gases, which can produce biases in simulated satellite radiances.

The measurement principle for emitted limb radiances is based on measuring the radiation emitted from the Earth's limb for a given tangent altitude against a space background. In contrast to the GPS measurements, this is a passive measurement technique, involving only an instrument onboard a single low-earth orbiting satellite. Current instruments using this technique are the Michelson Interferometer for Passive Atmospheric Sounding (MIPAS) flying on the Envisat satellite, and the Microwave Limb Sounder (MLS) onboard EOS-Aura. Past missions include the MLS on the Upper Atmosphere Research Satellite (UARS) and the Improved Stratospheric and Mesospheric Sounder (ISAMS) also on UARS.

Limb radiances provide additional information on temperature and the chemical composition of the stratosphere to lower mesosphere. The limb geometry means that the emitting material along the line-of-sight is maximised, and therefore even gases with low concentrations can be detected, and temperature can be measured at higher heights than typically possible with nadir sounders. The limb radiance assimilation in the ECMWF system aims to improve the analyses of humidity and ozone in the stratosphere, and to

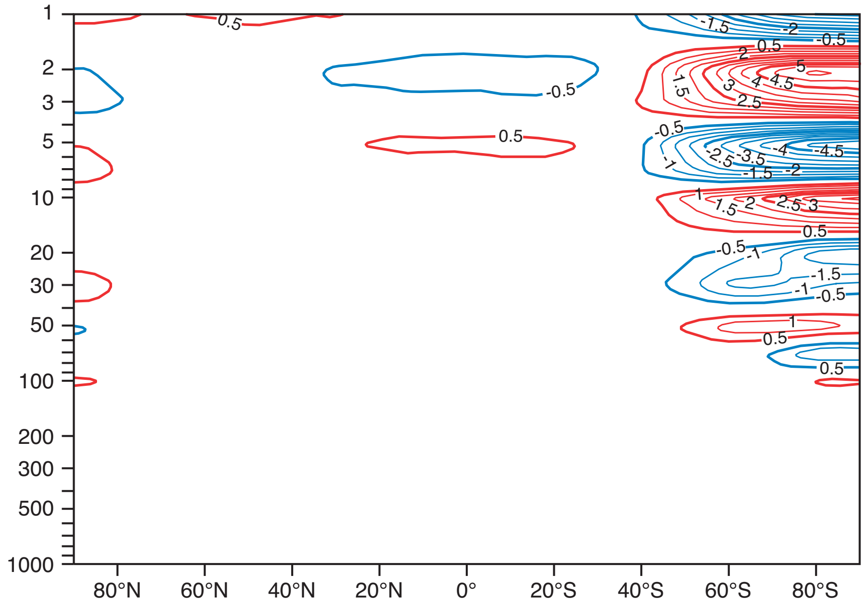

Figure 2 The zonally averaged mean differences in the CHAMP experiment minus the control temperature analyses, averaged over 1 June to 30 June, 2004.

add information on the vertical temperature structure in the stratosphere. It is the first time that limb radiances can be assimilated directly in an NWP model.

For both new types of observation we are assimilating a quantity that is as close as practical to the actual observations, instead of assimilating a retrieved profile derived by the data providers. This philosophy has proven very successful for the assimilation of data from nadir sounders at ECMWF and elsewhere, as it tends to simplify the specification of observation errors and biases. It also avoids the need to account for a priori information that might be used in the retrieval.

Limb observations are sensitive to the atmospheric conditions along the limb-viewing plane. This is a substantial difference to all other observations currently assimilated at ECMWF, as all other observations are mainly probing the atmosphere in a single profile. Considerable technical developments are underway to take into account the two-dimensional characteristics of the limb observations; as a first step we have performed assimilation experiments which assume that the limb observations are sounding a locally horizontally homogeneous atmosphere. In other words, these approaches use a single NWP profile at the assumed tangent point location to simulate the RO bending angles or limb radiances. Experimentation with this setup is ongoing, but the first results are looking very promising.

Experiments with RO data

In preparation for receiving GRAS and COSMIC data, a one-dimensional bending angle observation operator has been implemented in ECMWF's Integrated Forecasting System (IFS). The observation operator was developed by the EUMETSAT GRAS Satellite Application Facility (SAF) and it will be made available to the meteorological community. It has now been tested in a series of forecast impact experiments using CHAMP GPS RO measurements. CHAMP typically provides around 160 bending angle profiles per day and each profile contains approximately 160 bending angles. These data are assimilated without bias correction.

Despite the relatively low number of bending angles that are assimilated, the initial results have proved to be very encouraging. For example, Figure 2 shows the zonally averaged mean analysis differences of the CHAMP experiment minus the

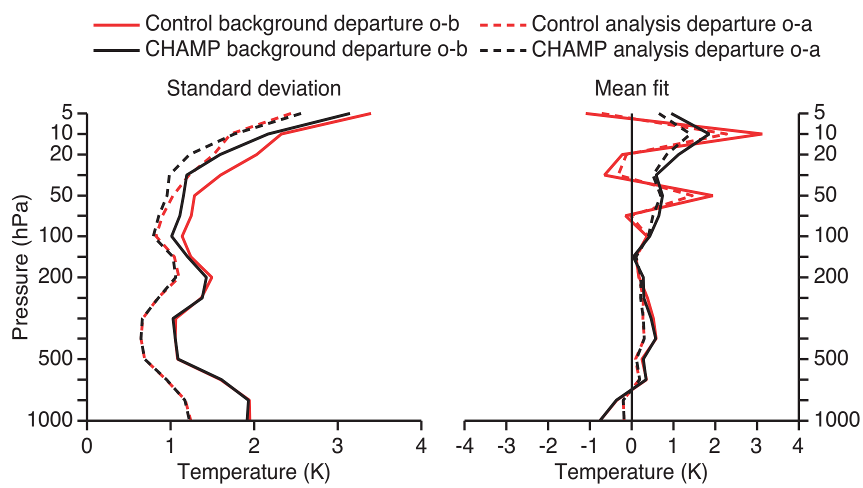

Figure 3 The mean and standard deviation of the background and analysis fit to radiosonde temperature measurements in Antarctica, from 1 June to 30 June, 2004.

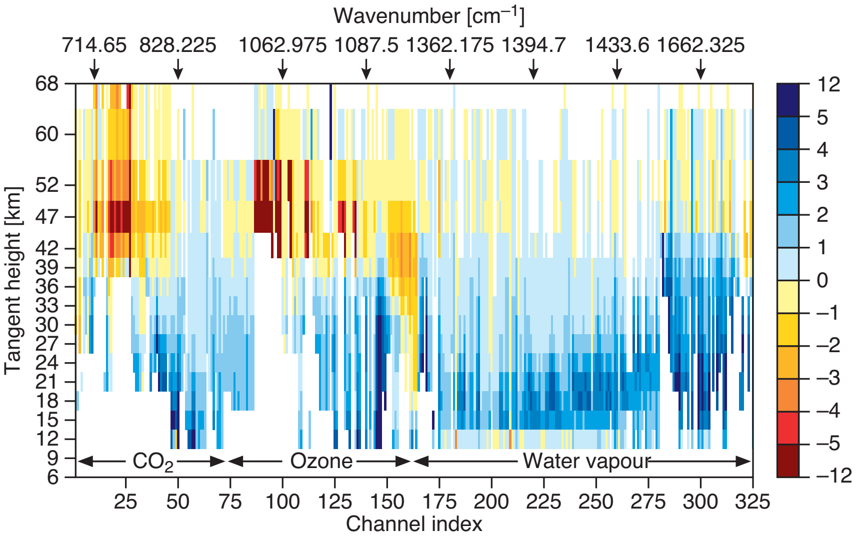

Figure 4 Bias between selected MIPAS clear-sky radiances and results simulated from short-term forecasts performed over the period 18–31 August 2003 from analyses without MIPAS data. The bias is shown as a function of channel index and tangent altitude. Wavenumbers (cm^{-1}) of some channels are indicated on the top axis for orientation purposes. The bias has been normalised by the MIPAS instrument noise.

control, for the period 1 June to 30 June, 2004. The control assimilates all the operational data that were used at that time; the CHAMP experiment is identical except for the use of CHAMP RO measurements in addition to these data. The most striking feature is over Antarctica, where there is a sharp, oscillatory structure in the mean analysis differences. The CHAMP GPS RO measurements improve both the mean and standard deviation of the background and analysis fit to radiosonde temperature measurements in this region, as illustrated in Figure 3. The "stratospheric ringing" in the mean fit to radiosondes over the winter pole is a well-known assimilation problem at ECMWF. The ability of the CHAMP data to introduce this kind of fine-scale structure, partially correcting these problems, is a clear indication of the accuracy and high vertical resolution of the measurement technique. More generally, assimilating the CHAMP measurements improves root-mean-square fit to lower-stratospheric radiosonde temperature measurements in the southern hemisphere, in the day-1 to day-5 forecast-range.

Experiments with limb radiances

The assimilation of limb radiances has been developed for data from MIPAS onboard the European Envisat satellite. MIPAS provides observations in the 685-2410 cm^{-1} region in 59,605 channels at very high spectral resolution (0.25 cm^{-1} in the original design). As it is unfeasible to assimilate data from all channels, we have selected a subset of MIPAS data with the aim to optimise the information content for a given number of observations.

The heart of the direct assimilation of limb radiances is a new fast radiative-transfer model that can simulate MIPAS radiances given the current state of the atmosphere (*Bormann et al.*, 2005). The development of this radiative transfer model has drawn heavily on the experience with fast radiative transfer modelling for nadir radiances accumulated at ECMWF and the NWP SAF over the last decade. The model is called RTMIPAS and it uses a regression approach, similar to that of the RTTOV fast radiative transfer model.

Comparisons between observed radiances and RTMIPAS-simulations highlight how MIPAS radiances detect large biases in the ECMWF model fields in the stratosphere. Figure 4 shows the bias between observed and simulated radiances, as a function of channel and tangent altitude, for a 14-day experiment during which MIPAS data were not assimilated. For a given tangent altitude, the sign of the bias is mostly the same for the majority of the channels considered. This consistency in the signal suggests that a large proportion of the bias is a result of biases in the model fields, since the weighting functions for most of the data shown in this figure peak around the tangent altitude. However, further work reveals, that some of the first guess bias shown in Figure 4 is also due to so-called radiance bias. This originates from inaccuracies in the spectroscopy used in the radiative transfer model, the calibration of the radiances, etc. Radiance biases need to be corrected prior to the assimilation, and the method used currently is similar to that employed operationally for AIRS nadir radiances. Developing approaches to separate between model and radiance biases is an area of active research.

The assimilation of MIPAS radiances leads to considerable changes in the mean analyses in the stratosphere, as the analysis aims to reduce the bias between model fields and observations. Figures 5 show the resulting changes in the mean analyses of temperature and humidity over a 14-day study period. Most noticeable is a moistening of the stratosphere. Assimilation of information on stratospheric humidity has recently become possible due to developments by *Hólm et al.* (2002), and MIPAS radiance assimilation provides a first test for these developments. Since so far no other observations are assimilated that provide information on stratospheric humidity it is hardly surprising that the assimilation of MIPAS data leads to such large adjustments for stratospheric humidity. Qualitatively, the adjustments introduced through the MIPAS radiance assimilation are in agreement with a known dry bias of the ECMWF stratosphere.

As a first check of whether the adjustments introduced through the radiance assimilation are reasonable, we have compared the model fields to ESA's MIPAS retrievals which were not used in the assimilation. These comparisons show that analyses with MIPAS radiances generally agree better with

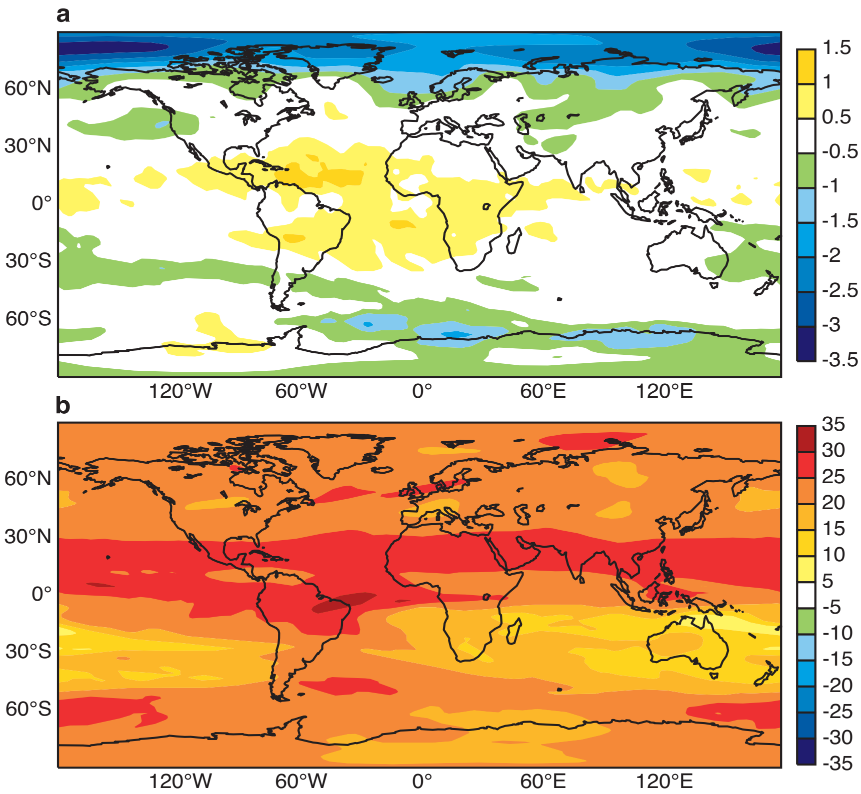

Figure 5 (a) Difference in the mean temperature analyses [K] at 5 hPa over the period 18–31 August 2003 between experiments with and without MIPAS radiance assimilation. (b) As (a), but for the relative difference in the mean humidity analyses [%] at 12 hPa.

MIPAS retrievals than analyses without MIPAS radiance assimilation (see Figure 6). This means that the information extracted by radiance assimilation is consistent with that provided through the MIPAS retrievals. This is an encouraging result, especially since the ESA retrievals have been derived separately from the ECMWF system from different subsets of MIPAS data and with a different radiative transfer model.

Comparisons between the analyses and other observations will be performed in the future to further evaluate the changes introduced through the MIPAS radiance assimilation. Unfortunately, few direct observations of stratospheric temperature, humidity and ozone are available, so retrievals from other satellite instruments may have to be used.

Use of two-dimensional observation operators

The forecast impact experiments using CHAMP bending angles and MIPAS radiances have been based on one-dimensional observation operators. This means that the simulated observations use NWP *profile* information at a single horizontal location. It is clear that ignoring the two-dimensional nature of limb measurements is an additional source of forward model error, which inhibits our ability to extract useful information. Therefore, ECWMF is currently investigating the use of two-dimensional observation operators for both measurement types. A two-dimensional version of RTMIPAS has been developed and extensively validated against simulated and observed radiances (*Bormann & Healy*, 2005). We have found that this substantially reduces the forward model error associated with horizontal gradients, for lower tangent altitudes and channels in strongly absorbing spectral regions. For these data, the line-of-sight weighting functions peak well away from the assumed tangent point, in the direction towards the receiver, thus increasing the sensitivity to horizontal gradients in the atmosphere.

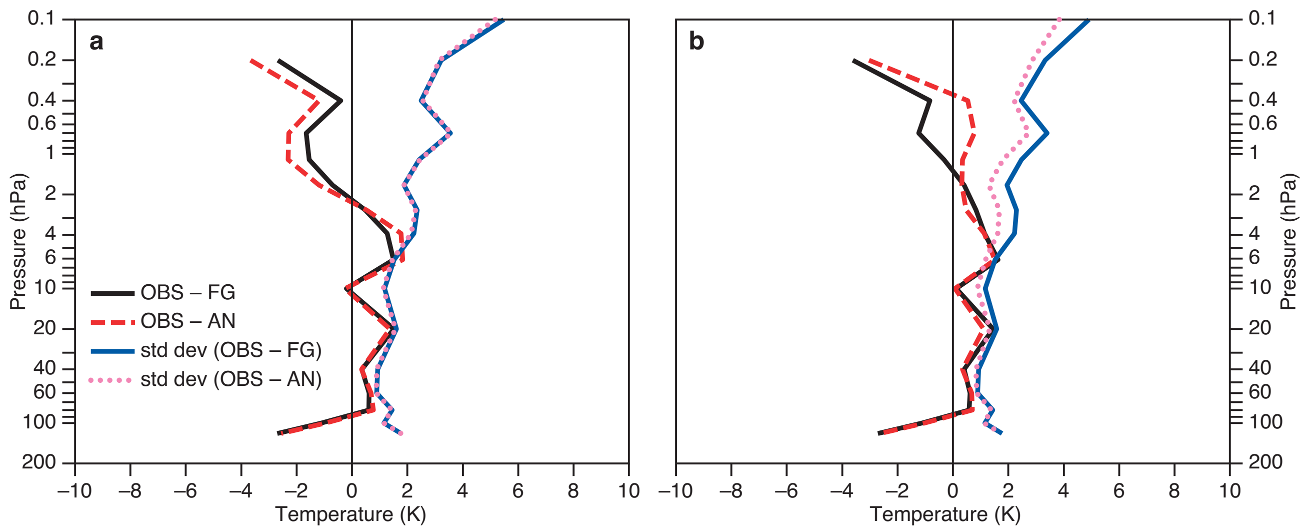

Figure 6 (a) First guess and analysis departure statistics for ESA's MIPAS retrievals over the southern tropics (0°–20°S) for an experiment without MIPAS radiance assimilation, covering the period 18–31 August 2003. (b) As (a), but for an experiment with MIPAS radiance assimilation.

In addition, we have started the first set of forecast impact experiments using a two-dimensional bending angle operator. This has involved significant restructuring and re-coding of the IFS by Mats Hamrud, in order to provide the GPS RO observation operator with information at a set of equally spaced horizontal locations, within the two-dimensional plane defined by the limb geometry of each occultation event. The preliminary results suggest that using the two-dimensional operator improves the root-mean-square fit to the observed bending angles by ~5%, for ray-paths close to the earth's surface, but this does not appear to have led to any clear improvement in the forecast scores. However, this is very much work in progress and further research is required.

Future work

The ultimate goal of this research project is the routine assimilation of limb measurements at ECMWF. We aim to operationally assimilate GPS RO bending angle measurements from CHAMP, GRAS and COSMIC during 2006. As MIPAS ceased routine operations in its original design in March 2004, the developments for the MIPAS limb radiance assimilation will primarily be used as a proof-of-concept study for limb radiance assimilation. Assimilation of MIPAS data over longer periods will allow a more detailed analysis of model behaviour and error characterisation in the stratosphere, for instance during the episode of the southern stratospheric vortex split in 2002. To this end, ECMWF is participating in the EU-funded ASSET project (Assimilation of Envisat DaTa) which will encompass intercomparisons of stratospheric analyses of chemical species produced with different assimilation systems and analysis methods. More generally, the developments for the assimilation of MIPAS radiances provide a framework for the assimilation of radiances from other limb sounders, such as the MLS on EOS-Aura.

FURTHER READING

Bormann, N. and **S. Healy**, 2005: A fast radiative transfer model for the assimilation of limb radiances from MIPAS: Accounting for horizontal gradients. *ECMWF Tech. Memo 468*, 24 pp.

Bormann, N., M. Matricardi, and **S. Healy**, 2005: A fast radiative-transfer model for the assimilation of infrared limb radiances from MIPAS. *Q. J. R. Meteorol. Soc.*, **131**, 1631–1653.

Healy, S., A. Jupp and **C. Marquardt**, 2005: Forecast impact experiment with GPS radio occultation measurements, *Geophys. Res. Lett.*, **32**, L03804, doi:10.1029/2004GL020806.

Healy, S. and **J-N. Thépaut**, 2005: Assimilation experiments with CHAMP GPS radio occultation measurements. *Q. J. R. Meteorol. Soc. (Accepted for publication).*

Hólm, E., E. Andersson, A. Beljaars, P. Lopez, J.F. Mahfouf, A.J. Simmons and **J-N. Thépaut**, 2002: Assimilation and modelling of the hydrological cycle: ECMWF's status and plans. *ECMWF Tech. Memo.* **383**, 55 pp.

Kursinski, E., G. Hajj, J. Schofield, R. Linfield and **K. Hardy**, 1997: Observing Earth's atmosphere with radio occultation measurements using the Global Positioning System. *J. Geophys. Res.*, **102**, 23,429–23,465.

Rocken, C., R. Anthes, M. Exner, D. Hunt, S. Sokolovskiy, R. Ware, M. Gorbunov, W. Schreiner, D. Feng, B. Herman, Y. Kuo and **X. Zou**, 1997: Analysis and validation of GPS/MET data in the neutral atmosphere. *J. Geophys. Res.*, **102**, 29,849–29,866.

Wickert, J., Ch. Reigber, G. Beyerle, R. König, C. Marquardt, T. Schmidt, L. Grunwaldt, R. Galas, T.K. Meehan., W.G. Melbourne and **K. Hocke**, 2001: Atmosphere sounding by GPS radio occultation: First results from CHAMP. *Geophys. Res. Lett.*, **28**, 3,263–3,266.

The local and global impact of the recent change in model aerosol climatology

Mark Rodwell

The impact of aerosol on local air quality and climate change is becoming an important topic of research. This is particularly the case for Asia where the so-called "Asian Brown Cloud" causes major health concerns and may have serious agricultural and economic consequences if aerosol can influence the climatological monsoon circulation. With these concerns in mind the ECMWF-coordinated "GEMS" project aims to improve our knowledge of atmospheric aerosol distribution (for further information see the article by Tony Hollingsworth in *ECMWF Newsletter No. 103*).

Here the impacts of a recent change in model aerosol climatology are investigated. It is found that the aerosol change (which is predominantly over North Africa) does influence the climatological North African monsoon circulation. In addition, it also has far wider impacts: affecting the winter extratropical circulation of each hemisphere and leading to improvements in medium-range forecast skill. These results suggest that the GEMS project could lead to further numerical weather prediction improvements and necessary advances in our understanding of climate change.

The old and new model aerosol climatologies

Until recently the aerosol climatology used in the ECMWF operational forecasting model (up to and including cycle Cy26r1) was based on that of *Tanre et al.* (1984). This climatology is specified as annual mean geographical distributions of various aerosol types: "maritime", "continental", "urban", "desert" and uniformly distributed stratospheric background aerosols, all with fixed vertical distributions. Figure 1(a) shows the geographical distribution of the total aerosol optical depth at 550 nm (an optical depth of *d* for a particular wavelength attenuates radiation at that wavelength by

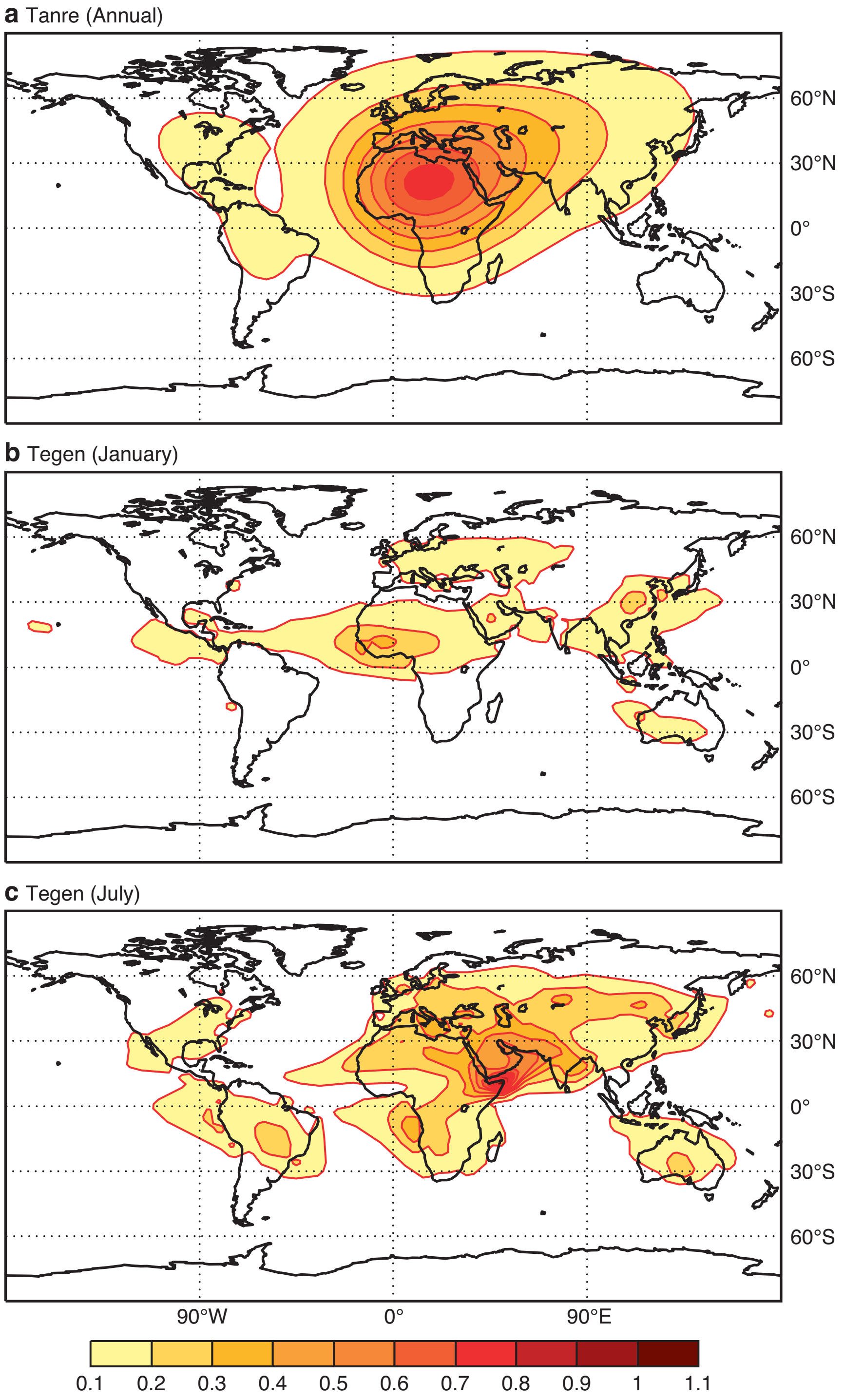

Figure 1 Optical depths at 550 nm associated with the model aerosol climatology. (a) The old annually-fixed climatology of *Tanre et al.* (1984). (b) The new January climatology of *Tegen et al.* (1997). (c) The new July climatology of *Tegen et al.* (1997).

a factor e^{-d} as it passes through the atmosphere). The maximum optical depth (0.74) is seen to occur over the Sahara and this is dominated by desert (sand dust) aerosol.

Over the last two decades, chemical and transport models, which are able to represent the life cycles of different aerosol types, have been used to create an inventory of their spatial and temporal distributions. Out of these studies, a new climatology for the annual cycle in each aerosol type has been compiled by *Tegen et al.* (1997). This climatology was implemented in the ECMWF forecast system at cycle Cy26r3 in October 2003. The new aerosol climatology for July (Figure 1(c)) is still dominated by sand dust but the region of maximum total optical depth (maximising at a value of 1.05) is now located over the Horn of Africa and out into the Arabian Sea associated with the transport of dust by the monsoonal Somali Jet. The aerosol optical depth over the Sahara is greatly reduced. The January aerosol of the new climatology (Figure 1(b)) also shows major differences with the old annual mean climatology (Figure 1(a)).

Tanre et al. (1984) investigated the impact of introducing aerosol into the ECMWF model; here the local and global impacts of the recent change in the aerosol climatology are discussed.

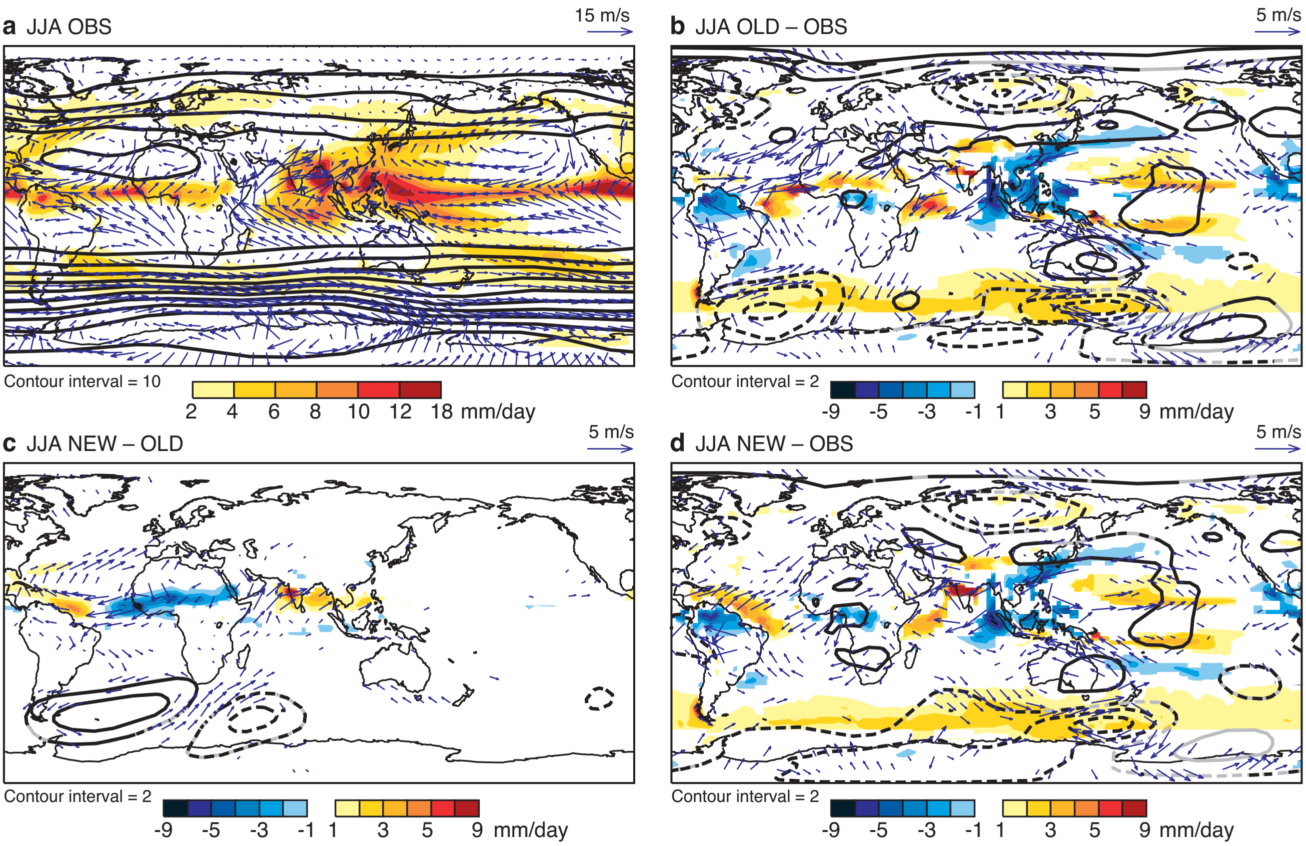

Figure 2 June–August total precipitation (shaded in mm day^{-1}), 925 hPa horizontal wind vectors (see scaling vector) and 500 hPa geopotential heights (contoured in dam). (a) From observations, with precipitation data coming from Xie-Arkin for the period 1980–1999 and the other fields from ERA-40 for the period 1962–2001. (b) Systematic error of model version Cy26r3 with old aerosol run at T95 resolution from 1 April for the years 1962–2001. (c) The difference between Cy26r3 with new aerosol and Cy26r3 with old aerosol. (d) Systematic error of model version Cy26r3 with new aerosol. Precipitation and wind differences are only plotted where they are statistically significant at the 10% level using a two-sided paired t-test taking autocorrelation into account. Height differences are contoured solid for positive, dashed for negative, grey where not significant and with contour interval indicated in each panel.

Impact on seasonal systematic errors (June–August)

Seasonal simulations have been made with the old and new aerosol, based on model version Cy26r3 run at T95 resolution and started from 1 April for the years 1962–2001 from ERA-40 analyses. Figure 2(a) shows mean June–August precipitation, low-level (925 hPa) winds and 500 hPa geopotential heights from the observations. The summer monsoons of southern Asia, North Africa and Mexico, together with their associated low-level inflows are clearly evident. In the extratropics, a weak (strong) westerly jet is evident from the tightness of the geopotential height contours in the summer (winter) hemisphere. The statistically significant systematic errors associated with the old aerosol (Figure 2(b)) include too much rain on the northern flank of the north African monsoon, strong wind biases over the sub-tropical north Atlantic and extratropical circulation biases to the southwest of southern Africa. The effect of the change in aerosol (Figure 2(c)) is a reduction in these particular biases so that they are no longer apparent in the systematic errors with the new aerosol (Figure 2(d)). Elsewhere, systematic errors are largely unchanged.

Impact on medium-range forecast skill (June–August)

The model version Cy26r3 (with new aerosol) was tested at T511 resolution during June–August 2003 alongside the then operational version Cy26r1 (with old aerosol). Significant medium-range anomaly correlation skill improvements are apparent throughout the tropics in Cy26r3. Although there are several differences between these two analysis/model cycles, the major improvements in, for example, 925 hPa temperature over northern Africa (Figure 3(a)) (where a gain of 1.5 days is apparent for an anomaly correlation of 0.6) and in 925 hPa zonal wind over the subtropical north Atlantic (Figure 3(b)) (gain of 0.4 days) would appear to be predominantly due to the change in aerosol.

Understanding the local improvements

To better understand the physics that leads to these improvements it is useful to study the mean forecast "spin-up". If the model is not perfect, it is likely to have a somewhat different mean climate to that of the real world (or of the analyses). When averaged over many forecasts, the tendencies in the first few timesteps will reflect the adjustment from the climate of the analysis to the climate of the model. Moreover,

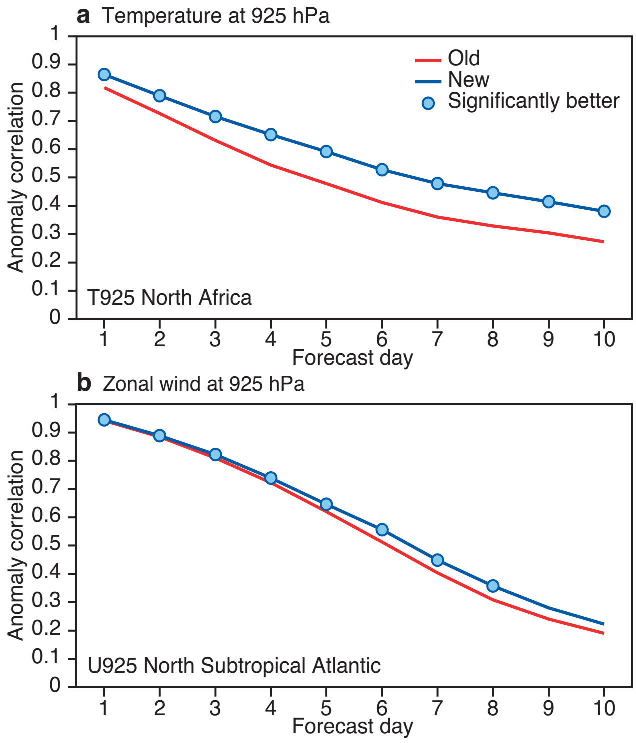

Figure 3 Mean anomaly correlations from T511 medium-range forecasts started each day in June–August 2003. (a) Temperature at 925 hPa over North Africa (20°W–40°E, 0°N–25°N). (b) Zonal wind at 925 hPa over the north subtropical Atlantic (80°W–10°W, 0°N–45°N). Red for the analysis/model version Cy26r1 (with old aerosol) and blue for Cy26r3 (with new aerosol). Dots indicate statistically significantly better forecast skill at the 10% level using a two-sided paired t-test taking autocorrelation into account.

since individual schemes within the model (convection, radiation, dynamics etc.) have not had time to fully interact with each other in the first few timesteps, it may be possible to break-down the complex physics involved in this adjustment and even identify the reasons for errors in the model climate.

To isolate the tendencies involved in the adjustment, one needs to remove the tendencies associated with the diurnal cycle. *Klinker and Sardeshmukh* (1992), who have previously used this "tendency budget" technique, removed the diurnal cycle by averaging the tendencies of forecasts started at four different times of the day (starting at 0, 6, 12 and 18 UTC). Tendency budget analysis was dropped when 4D-Var data assimilation was introduced because it was thought that the analysis would be too close to a valid model state to be able to detect any adjustment. This is partly the case (at least for the Amazon region that has been investigated in this respect) especially with a 12 hour (rather than 6 hour) data assimilation window. However by sampling the diurnal cycle more frequently it has been possible to estimate the adjustment more precisely and thus still use the methodology.

The mean tendencies are obtained from medium-range forecasts using model version Cy28r3 T255L60 with old and new aerosol. Forecasts were started every fifth day within June-August for 2003 and 2004 (a total of 38 forecasts) from operational analyses. These years were chosen because analyses in 2003 were made when the old aerosol was in operation and those in 2004 were made when then the new aerosol was in operation. Thus neither aerosol climatology should be favoured by the analysis. Diurnal averaging of "initial tendencies" is done between D+0.25 and D+1.25 and diurnal averaging of "balanced tendencies" is done between D+9 and D+10. Figure 4 shows vertical profiles of tendencies from the dominant schemes within the models, together with the total tendencies and the D+10 biases, averaged over the North African box 10°W–30°E, 5°N–30°N.

- Left column — initial temperature tendencies (D+0.25 to D+1.25).
- Middle column — balanced temperature tendencies (D+9 to D+10).
- Right column — initial humidity tendencies (D+0.25 to D+1.25).
- Top row — model with the old aerosol.
- Middle row — model with the new aerosol.
- Bottom row — difference between models with new and old aerosols (note the change in horizontal axis scaling).

All profiles include 70% confidence intervals (which take autocorrelation into account).

To a large extent, the initial temperature tendencies (Figure 4(a)) associated with the individual physical schemes balance each other. For example, in the mid-troposphere, convective heating (blue) tends to balance radiative cooling (dark green). This is an example of radiative-convective equilibrium. However, the total of the individual tendencies (red) is not quite zero and this reflects the climate adjustment. The tendency is for a warming of the lower troposphere (below about 500 hPa) and this is reflected in the D+10 bias (black) (although not below 884 hPa for which the bias must either develop before D+0.25 or after D+1.25: this is an important topic for future investigation and not affected by the aerosol change). The initial balance in lower-tropospheric humidity tendencies (Figure 4(c)) is between convective removal (blue) and dynamic supply (orange). Again the balance is not perfect and there is an initial moistening of the lower troposphere (red) which is clearly reflected in the D+10 bias (black). The destabilization of the upper-tropospheric thermal profile and stabilisation below (which is what one would expect intuitively from an excessive amount of aerosol) is likely to be the cause for the moistening of the lower troposphere and, in the balanced profiles (Figure 4(b)), the strong increase in upper-tropospheric convective heating (blue) and dynamical cooling (orange).

The total tendencies (and D+10 biases) from the model with the new aerosol (Figure 4, middle row) are generally much better than with the old aerosol (Figure 4, top row). In particular, the initial mid-tropospheric warming and D+10 warm bias have disappeared, the initial lower tropospheric moistening and D+10 moisture bias are halved and the balanced temperature tendencies are much more similar to the initial tendencies than was the case with the old aerosol.

The profile differences (Figure 4, bottom row) can help explain these improvements. The reduction in aerosol leads to less tropospheric shortwave absorption and more near

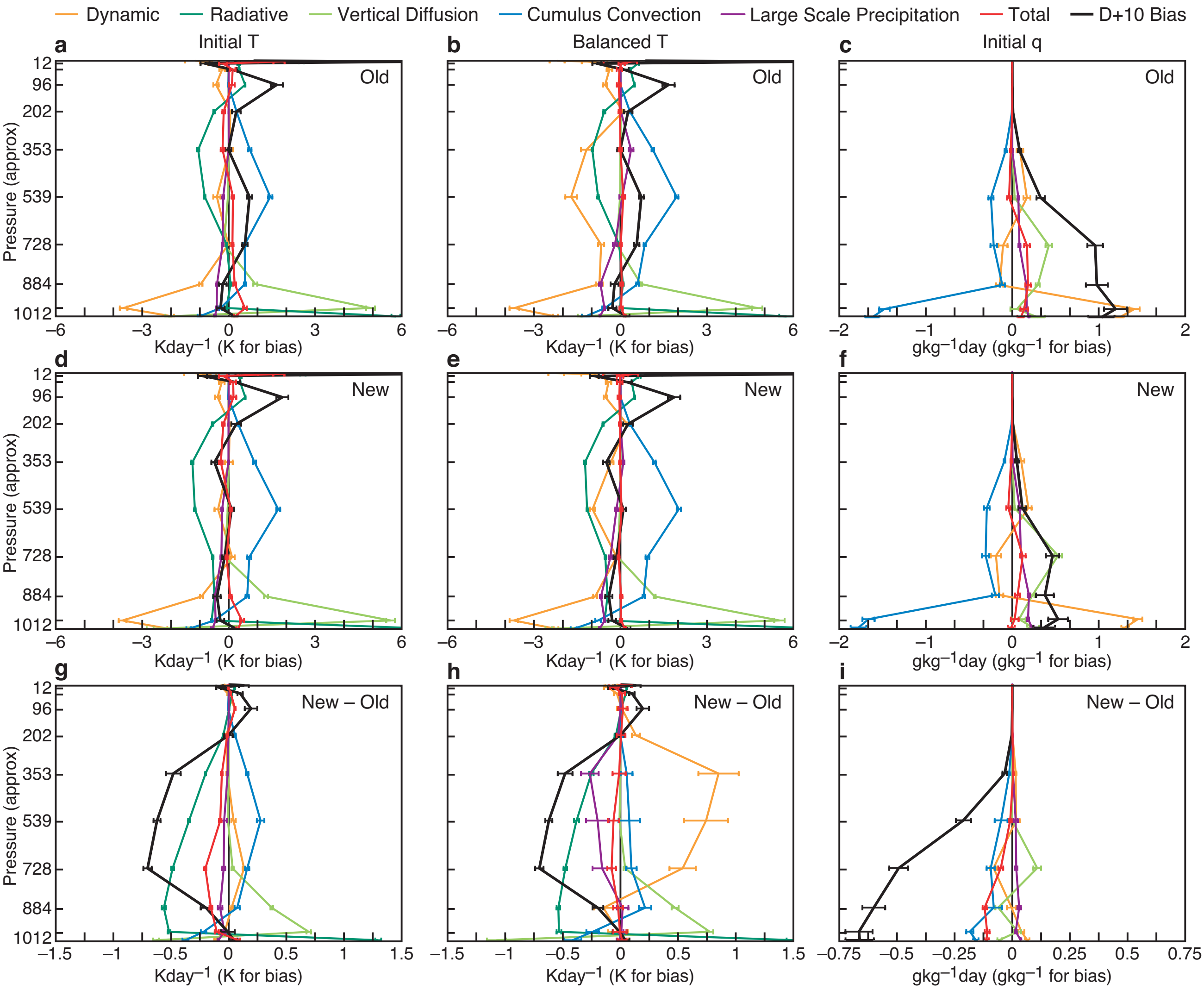

Figure 4 Vertical profiles of mean tendencies from the dominant physical schemes and the dynamics, together with total tendencies and D+10 biases (see key). 70% confidence intervals are indicated (taking autocorrelation into account). Model-level tendencies are obtained from 38 T255L60 forecasts started every fifth day during June-August for 2003 and 2004. The vertical axis shows approximate model level pressure and is linear in pressure. See captions or the main text for an explanation of the individual panels.

surface heating (Figures 4(g) and 4(h), dark green). The initial differences for the other schemes are non-zero (Figure 4(g)). This indicates that over the first day these schemes have already begun to partially balance the radiative heating change. Nevertheless, the total tendency change (red) and D+10 bias change (black) do reflect the radiative forcing change. The destabilisation of the lower troposphere lowers the level from which initial convection can start and thus the convection is better able to remove the moisture supplied by the dynamics. Figure 4(i) shows this increased convective removal of moisture (blue) and the dramatic improvement in the D+10 biases (black).

An increase in convection throughout the troposphere (seen in the balanced temperature profile change, Figure 4(h), blue) may seem counter-intuitive since we have seen that the total precipitation actually decreases with the new aerosol (in these experiments D+10 area-mean precipitation reduces from 3.8 mmday^{-1} to 2.9 mmday^{-1}, with an observed value from GPCP data of 2.7 mmday^{-1}). However, the increase in convection "feeds-off" the destabilised thermal profile and thus cannot entirely negate the radiative cooling effect of the aerosol change. Thus with the new aerosol there must be more descent (or less ascent), less large-scale moisture convergence and a reduction in large-scale precipitation. For moisture conservation, the reduction in large-scale precipitation must more than balance the increase in convective precipitation. All these features are evident in the balanced temperature profile changes (Figure 4(h)).

D+10 zonal and meridional wind bias profiles (not shown) are also substantially (and statistically significantly) improved with the new aerosol. For example the 202 hPa meridional wind bias is reduced from −1.7 ms^{-1} to −0.2 ms^{-1} and the 884 hPa bias is reduced from +1.6 ms^{-1} to +0.8 ms^{-1}. These changes are consistent with the "local Hadley Circulation" change associated with the weakening and southward shift of the North African monsoon/ITCZ circulation. Further insight into the impact on the African Easterly Jet can be found in *Tompkins et al.*, 2004.

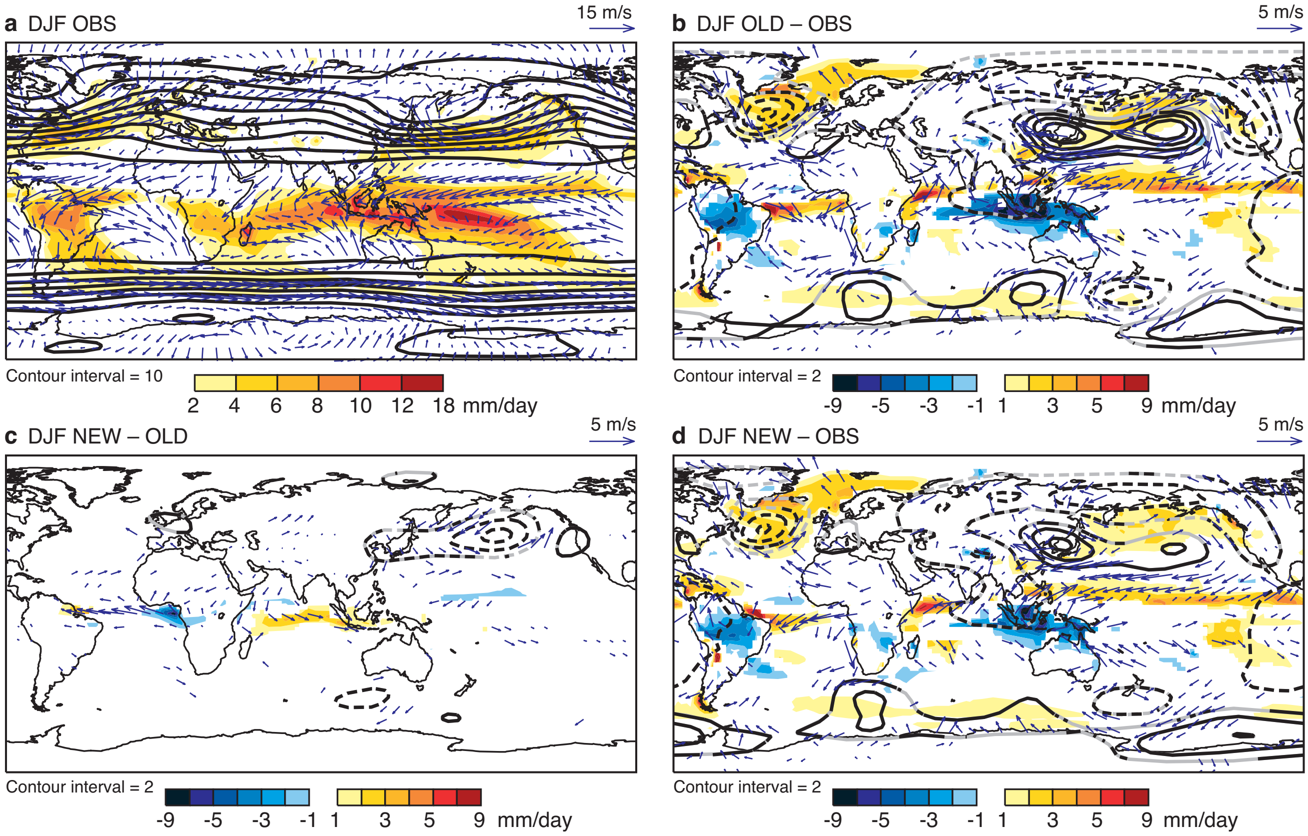

Figure 5 December–February total precipitation (shaded in mmday^{-1}), 925 hPa horizontal wind vectors (see scaling vector) and 500 hPa geopotential heights (contoured in dam). (a) From observations, with precipitation data coming from Xie-Arkin for the period 1979/80–1998/99 and the other fields from ERA-40 for the period 1962–2001. (b) Systematic error of model version Cy26r3 with old aerosol run at T95 resolution from 1 October for the years 1962–2001. (c) The difference between Cy26r3 with new aerosol and Cy26r3 with old aerosol. (d) Systematic error of model version Cy26r3 with new aerosol. Precipitation and wind differences are only plotted where they are statistically significant at the 10% level using a two-sided paired t-test taking autocorrelation into account. Height differences are contoured solid for positive, dashed for negative, grey where not significant and with contour interval indicated in each panel.

The tendency budget method provides a powerful and objective method of assessing changes to the model physics. Although a detailed analysis of the effects of the aerosol change has been given above, it should be noted that a simple assessment of the total initial tendencies is all that is required to determine whether a particular physics change is good or bad. Ideally, a separate data assimilation cycle should be made for each model version and each model initiated with its own analysis. This was not considered necessary here for the reasons stated above.

Impact on seasonal systematic errors (December–February)

Figure 5 shows climate simulation results for the December-February season based on forecasts started on 1 October for the years 1962–2001. The monsoons are now in the Southern Hemisphere (Figure 5(a)). The biases in the simulations with the old and new aerosols are shown in Figures 5(b) and 5(d), with the difference in the biases given in Figure 5(c). These results indicate that the aerosol change improves the precipitation biases over the tropical Atlantic and Indian Ocean, and (rather curiously due to its apparent disconnectedness) the height bias over the North Pacific. During this season the change in aerosol has a strong local impact on precipitation over the Gulf of Guinea. This is because, over the ocean, the atmospheric cooling associated with the reduced absorption of solar radiation is not balanced by surface sensible (or latent) heat fluxes as the ocean has a high heat capacity (it is infinite in these prescribed SST experiments). The dynamic adjustment to this cooling reduces the amount of moisture available to precipitate. The increase in precipitation to the east, over the Indian Ocean is consistent with an eastward upwelling Kelvin wave response to the Gulf of Guinea latent heating change although an additional local response to aerosol changes over the Indian Ocean itself has not been ruled-out at present.

Understanding the global improvements

To better understand the North Pacific pressure bias improvement, Figure 6 shows 250 hPa seasonal simulation differences (new minus old aerosol) in stream function (thick contoured), divergent wind (vectors) and "Rossby Wave Source" (shaded), *Sardeshmukh and Hoskins* (1988). The anomalous upper-level convergence over the Gulf of Guinea, associated with the precipitation decrease, and divergence over the Indian Ocean (and associated convergence to the north) are clearly evident. In addition, the strong reduction in aerosol over the Sahara (compare Figures 1(a) and 1(b)) leads to a radiative cooling

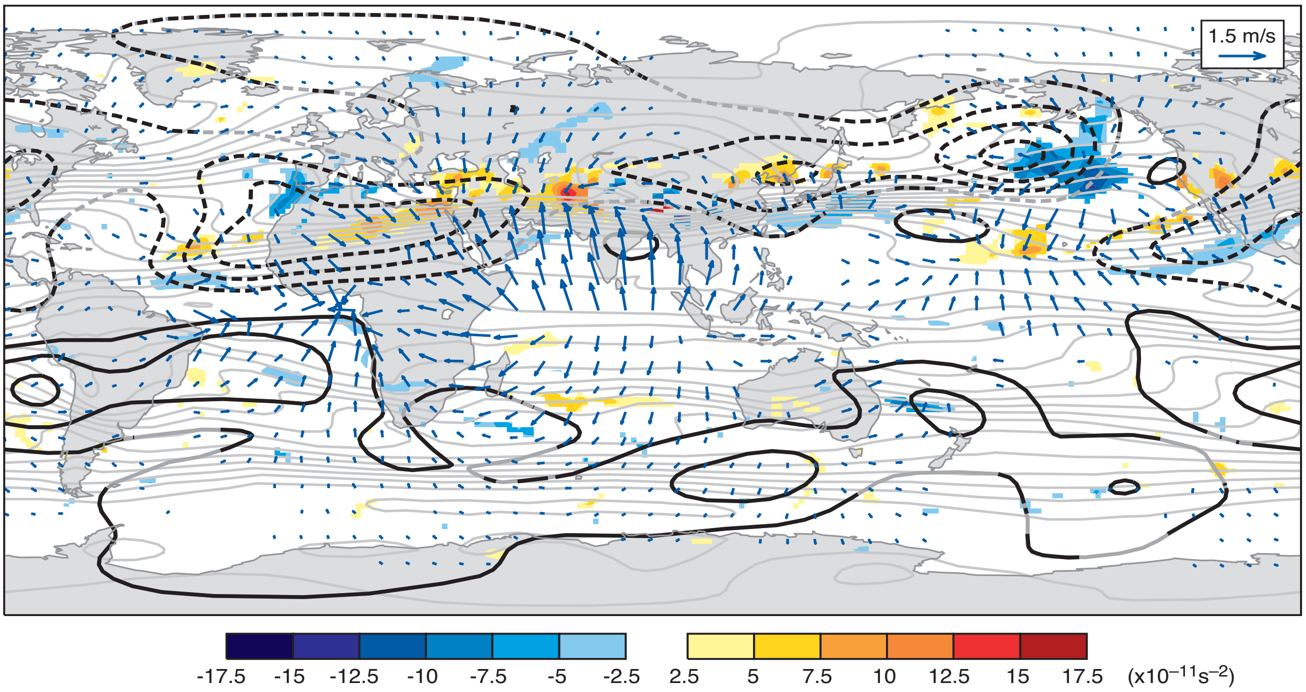

Figure 6 The difference between Cy26r3 with new aerosol and Cy26r3 with old aerosol in terms of the 250 hPa divergent wind vectors, stream function (contoured thick – contour interval 2×10^6 m^{2}s^{-1}) and Rossby Wave Source (shaded – contour interval of 2.5×10^{-11} s^{-2}). Also shown is the mean (i.e. (old+new)/2) absolute vorticity (contoured thin grey with interval 1×10^{-5} s^{-1}). Differences in divergent wind and Rossby Wave Source are only plotted where significant at the 10% level. Streamfunction differences are contoured solid where positive, dashed where negative and grey where not significant.

anomaly (not shown). Although there is no precipitation for this forcing to positively feed-back with at this time of year, the radiative cooling alone is apparently enough to force considerable descent and upper-level convergence. The upper-level divergence field associated with all these features and the advection of mean absolute vorticity (mean absolute vorticity is shown with thin grey contours) by the divergent wind leads to Rossby wave forcing (shading) along the Northern Hemisphere subtropical jet. The apparently disconnected North Pacific pressure bias improvement is now seen (rather beautifully!) to be part of the barotropic Rossby wave response to this vorticity forcing.

Note that for June–August, the tropical upper tropospheric stream function and Rossby Wave Source biases are greatly improved with the new aerosol; with the remaining source of error centred around the Philippine Sea region (not shown). The extratropical responses for both June-August (Figure 2) and December-February (Figure 5) are predominantly limited to the winter hemisphere. It is possible that the upper-level out-flow associated with tropical convective anomalies is stronger in the winter hemisphere (as is the case for the mean Hadley Circulation) and has a stronger impact on vorticity forcing owing to the stronger winter vorticity gradients.

Future use of observed and interactive aerosol

We have seen that changes in aerosol can have a strong impact on local precipitation and the global circulation. This effect is apparent not only in seasonal forecasts but also in the medium-range. This being so, what would be the impact of using observed aerosol? Seasonal forecast sensitivity experiments have been carried out in which the new (Tegen) aerosol was replaced with MODIS satellite-derived aerosol optical depths. Over Asia this did not lead to such large changes in the local or global circulation in June-August. This may reflect the smaller and more local change in aerosol or highlight the importance of a strong interaction with precipitation in order to magnify the aerosol effect. Nevertheless, the results above indicate that it is possible that the future use of observed aerosol and the incorporation of an interactive aerosol scheme could lead to further forecast skill improvements.

FURTHER READING

Klinker, E. and **P.D. Sardeshmukh**, 1992: The diagnosis of mechanical dissipation in the atmosphere from large-scale balance requirements. *J. Atmos. Sci.*, **49**, 608–627.

Sardeshmukh, P.D. and **B.J. Hoskins**, 1988: The generation of global rotational flow by steady idealized tropical divergence. *J. Atmos. Sci.*, **45**, 1228–1251.

Tanre, D., J-F. Geleyn and **J.M Slingo**, 1984: First results of the introduction of an advanced aerosol-radiation interaction in the ECMWF low resolution global model. In *Aerosols and Their Climatic Effects*. H.E. Gerber and A. Deepak, Eds., A. Deepak Publ., Hampton, Va., 133–177.

Tegen, I., P., Hollrig, M. Chin, I. Fung, D. Jacob and **J. Penner**, 1997: Contribution of different aerosol species to the global aerosol extinction optical thickness: Estimates from model results. *J. Geophys. Res.*, **102**, 23895–23915.

Tompkins, A.M., C. Cardinali, J-J. Morcrette and **M.J. Rodwell**, 2004: Influence of aerosol climatology on forecasts of the African Easterly Jet. *Geophys. Res. Lett.*, **32**, doi:10.1029/2004GL022189.

Ocean analysis at ECMWF: from real-time ocean initial conditions to historical ocean reanalysis

Magdalena A. Balmaseda, David Anderson and Arthur Vidard

Global ocean analyses are performed daily at ECMWF to provide ocean initial conditions for both monthly and seasonal forecasts. Although the analysis systems have many features in common, they are not identical because of the greater time constraints imposed by the monthly system. Daily analyses have been produced routinely at ECMWF since 1997 as part of the seasonal forecasting system. These analyses are produced 12 days behind-real-time (BRT). The delay is required partly to allow receipt of data, and partly because the data window used in the analysis is 10 days (5 days before and after the analysis time). In 1997, an appropriate delay for receipt of data was 6 days. Now, most subsurface data are received within a day or two but there is still a delay of up to 12 days in obtaining a quality sea surface temperature (SST) analysis. While a delay of 12 days in producing initial conditions for a 6-month forecast might be quite acceptable, it is inadequate for a monthly forecast: an up-to-date analysis is required. To this end, an early delivery ocean analysis system was introduced in May 2004. It generates daily near-real-time (NRT) analyses of the ocean and runs only 8 hours behind-real-time.

Figure 1 shows schematically the schedule followed in the production of the NRT and BRT ocean analyses. Every day, the NRT ocean analysis is produced by starting from the latest BRT analysis and integrating the ocean model up to real time (i.e. 12 days forward), using all the available observations during that period. During the 12 days there are two assimilation cycles. The first assimilation takes place 12 days behind-real-time (D-12), using a 10-day window centred at D-12, and the second assimilation is performed at D-2, using observations from a 7-day off-centred window as shown in Figure 1. Except for the schedule and number of observations, both BRT and NRT products are generated with the same ocean analysis system (described below). Global three-dimensional fields of temperature, salinity and velocity for the upper ocean are produced with a horizontal resolution of approximately 1° in the extratropics, increasing to ⅓° meridionally in the equatorial region. The vertical resolution in the upper 100 m is ~10 m. In addition to the three-dimensional fields there are analyses of two-dimensional fields such as sea level and mixed-layer depth.

In addition to the ocean initial conditions for the real-time coupled forecasts, ocean reanalyses for an extended historical period are also produced at ECMWF. These are needed to initialize the retrospective coupled hindcasts that are used for the calibration of the coupled model output and for skill assessment. It is important that the historical ocean analysis provides a reliable representation of the climate variability and consistency between the historical and the "real-time" products is also required. The BRT ocean analysis can be considered as part of the historical ocean analysis that continues producing consistent analysis products close to real time, unlike the atmospheric reanalyses that generally stop production at a given date (ERA-15 products exist until 1994, and ERA-40 ended on 31 December 2002).

The rest of the article gives more detail about the ocean analysis system and ocean observations, and considers the importance of ocean initial conditions for extended range forecasts. Also the work on producing ocean reanalyses to provide initial conditions for the calibration of coupled model forecasts is described. Finally there is a description of plans to upgrade the ocean analysis system together with the seasonal forecasting system later this year.

The ocean analysis system

The scheme currently in operational use is OI (Optimal Interpolation), with a time window of 10 days; all the observations in the 10-day window are applied at the centre of the window. It differs from a standard OI, however, in that the resulting correction to the first guess (FG) is not applied instantaneously; rather the correction is applied incrementally during the subsequent 10 days. The FG is provided by forcing an ocean model with daily fluxes of momentum, heat, and fresh water from the NWP atmospheric analysis system. The ocean model in use is HOPE (Hamburg Ocean Primitive Equations).

Only subsurface temperature observations are assimilated presently, but corrections are applied to the temperature, velocity and salinity fields. Salinity is corrected by invoking the conservation of the water mass characteristics, in particular the relationship between temperature and salinity. The geostrophic velocity derived from the temperature and salinity increments is then applied as a correction to the velocity field.

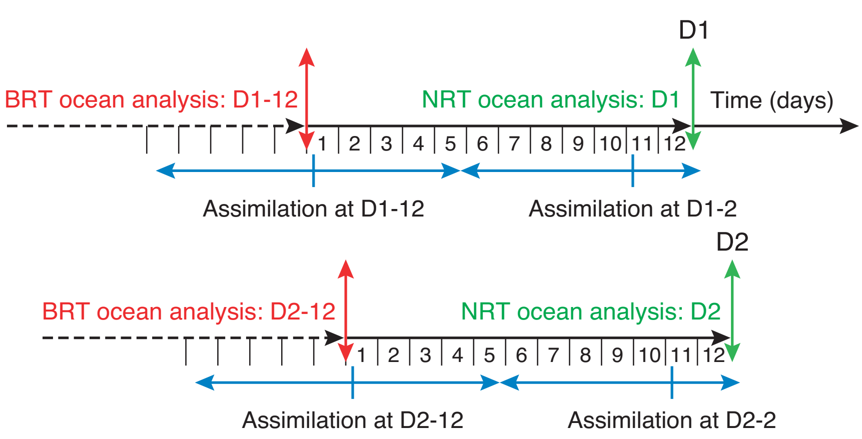

Figure 1 Schedule followed in the production of the near-real-time (NRT) and behind-real-time (BRT) ocean analysis.

An important feature of the ECMWF ocean analysis system is that not just a single analysis but several simultaneous analyses are performed. The purpose of the multiple analyses (five in total) is to sample uncertainty in the ocean initial conditions. The ensemble of ocean initial conditions provided by the five analyses contributes to the creation of the ensemble of forecasts for the probabilistic predictions at monthly and seasonal ranges. The five simultaneous ocean analyses are created by adding perturbations, commensurate with the estimated uncertainty, to the wind stress while the model is being integrated forward from one analysis time to the next.

The ocean observations

Over the last decade the number of oceanic observations available in near-real-time has increased considerably. Also the number of observing systems has increased.

Types of observations

Subsurface temperature observations are currently provided by the TAO/TRITON and PIRATA arrays in the equatorial region and the global Volunteer Observing Ship (VOS) programme which provides XBT (eXpandable Bathythermograph) measurements mainly along merchant shipping routes. More recently, observations are provided by the ARGO network of drifting profilers. The drifters frequently provide salinity measurements and, while these are not assimilated in the current system, they will be used in the next upgrade of the operational system, due later this year. Likewise altimeter-derived sea level anomalies are not currently assimilated but will be in the next operational system. The salinity and altimeter data are currently used for validation purposes. There are no real-time measurements of velocity, except in the surface layer. Delayed mode velocity measurements are used for validation purposes. Daily SST maps, derived from the time interpolation of weekly SST products from NCEP, are used to constrain the temperature of the model surface layer.

The mooring array consists of TAO moorings in the central Pacific, TRITON moorings in the west Pacific, and PIRATA moorings in the tropical Atlantic. In the different regions the moorings are broadly similar although there are differences in their operational characteristics. Figure 2(a) shows a TAO/ATLAS mooring. The TAO network provides in-situ temperature observations down to a depth of 500 m on a daily basis for the equatorial Pacific. The moorings are arranged on a grid spanning the equatorial Pacific between 8°S and 8°N, and the longitudinal gap between buoys is typically 1500 km. In the meridional direction, buoys are located at approximately 8°S, 5°S, 2°S, 0°, 2°N, 5°N and 8°N. Thermistor chains with sensors at fixed depth are carried by the buoys: typically at the surface, 25, 50, 75, 100, 125, 150, 200, 250, 300, and 500 m. Data are transmitted as daily averages from samples taken 10 minutes apart. The TRITON moorings, located west of the date line, are also part of the Pacific array but their transmission characteristics are different to TAO. Namely they provide an additional measurement at 750 metres, they report hourly, and the profiles are not always transmitted as whole profiles. There are some TAO and TRITON moorings in the Indian Ocean with planned

a

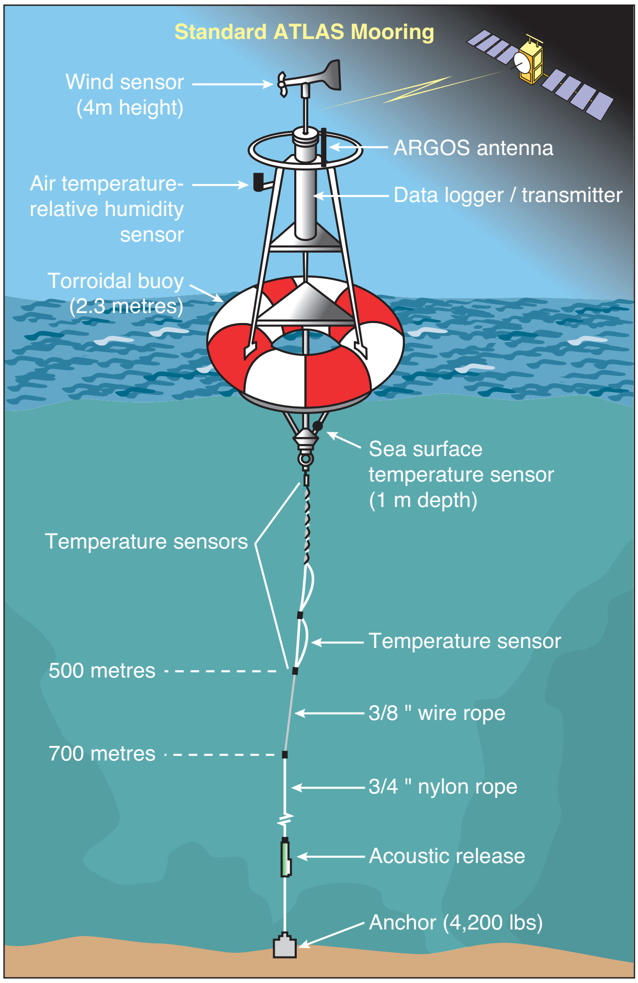

b

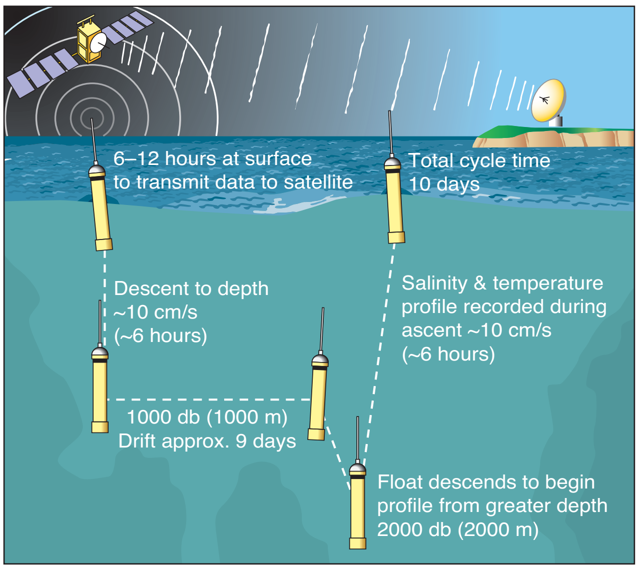

Figure 2 (a) Scheme of an ATLAS mooring (www.pmel.noaa.gov). (b) Working scheme of the ARGO floats (www.argo.ucsd.edu).

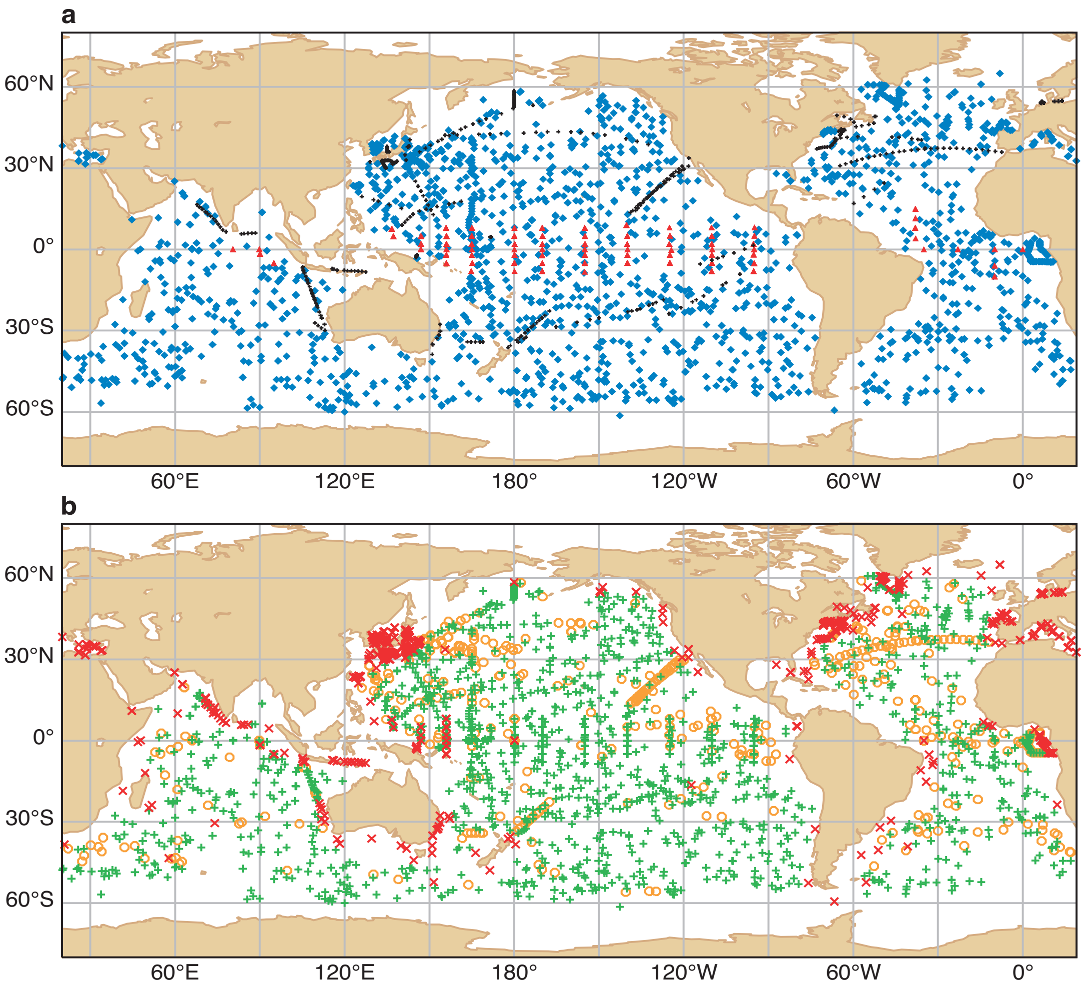

Figure 3 (a) Spatial coverage of the observations used in the delayed ocean analysis for a typical 10-day period, showing the TRITON/TAO/PIRATA mooring array in the Pacific/Atlantic oceans (▲), the XBT network (+) and the ARGO floats (◆). (b) Profiles that have been accepted after the quality control procedure are marked as + and those that are rejected as ×. Profiles where part was accepted and part rejected are marked as ○. Data close to coasts are rejected automatically.

extensions. The Atlantic array covers a broader latitudinal extent than the Pacific.

The XBTs provide measurements which can go down to 800 m. These observations provide better vertical resolution than the TAO data, but are irregular in space and sparse in time. The network is not specially designed to observe the equatorial Pacific, and the number of frequently-observed tracks crossing the equator is relatively low. In the last few years the number of XBTs lines has been decreasing.

The ARGO profiling floats are the most recent of the observing systems. Deployment started in the late 1990s. About 170 floats were reporting in 2001: this increased to over 800 by mid 2003 and currently the number of floats is close to 2,000. It is expected that by 2006 there will be 3,000 floats distributed over the global oceans at three-degree spacing. Measurements of temperature and salinity down to 2000 m depth are provided every 10 days. The buoys drift at ~1000 m for 9 days, and on the 10th day they descend to 2000 m before starting to rise to the surface, measuring temperature and salinity on their way up; they then transmit the information via satellite (Figure 2(b)).

Distribution and number of observations

Figure 3(a) shows the spatial coverage of subsurface temperature observations used by the delayed analysis in a typical 10-day window. The TRITON/TAO/PIRATA mooring array is represented as red triangles, the XBT network as black crosses and the ARGO floats as blue diamonds. Most of the data are now received at ECMWF within one day or so, through the Global Telecommunications System (GTS). When data are received they are subjected to an automatic quality control procedure: each individual observation is checked and compared against the model first guess and also with an analysis performed without the datum being checked (buddy check). Figure 3(b) shows the quality control decisions: the rejected data appear in red, the accepted data in green and partially accepted in orange. Since coastal areas are not well represented by the ocean model the data near the coast are rejected. In open ocean some profiles are partially rejected; at some depths the model and observations differ too much and the data are rejected, but data from the same profile above or below might be used. The quality control also has a super-obbing scheme: if there are many data points in close proximity in space and time, they are combined into a "super-observation" and given increased weight. After the quality control, about 15% of the profiles are rejected, 15% partially accepted and 70% fully accepted, of which more than 50% are super-obbed.

Timeliness of observations

As mentioned earlier, during the 12 days that it takes to bring to real time the NRT ocean analysis, there are two assimilation cycles. The first is at the beginning of the 12-day integration, i.e. 12 days behind-real-time (D-12). This analysis uses the observations in a centred 10-day window. The data in this first assimilation window is about the same as that used in the delayed analysis centred on the same date. The second assimilation is performed 2 days behind-real-time (D-2). For this cycle, the observation window spans a 7-day range, and is off-centred (5 days before, 2 days after the analysis time). Figure 4 shows the number of observations used in this second assimilation, classified by observing system and compared with the number of observations for the same date in the delayed analysis. The number of observations in the second assimilation of the NRT analysis is smaller, as expected from the shorter window, but the number of observations is more or less proportional to the number of days since most observations are now received within one day.

The arrival of SST information is one of the major factors for introducing a delay in the analysis. Global SST maps from NCEP are received every Monday at midday, representing the average of the previous week SST values. For the delayed ocean analysis, daily SST maps are obtained by interpolation of the weekly products, which requires the existence of two consecutive weekly values. This can introduce a delay of up to 12 days. The NRT analysis does not wait for the second map of SST to be available. Instead, a daily SST product is created by adding the latest SST anomaly to the daily climatology. The importance of representing daily variations of the annual cycle in SST is illustrated in the next section.

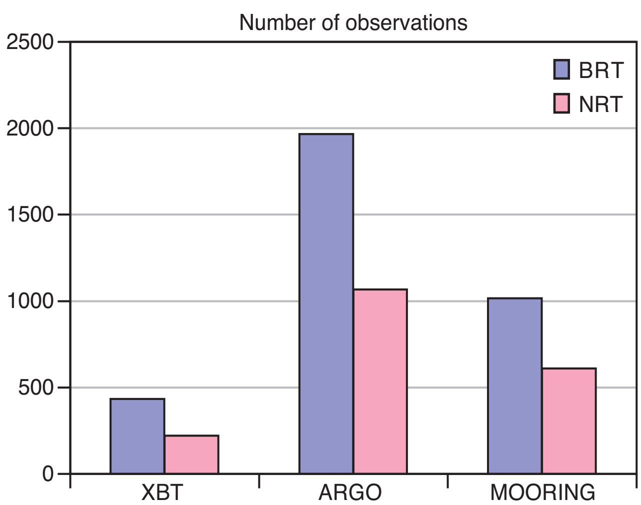

Figure 4 Number of observations received in a standard 10-day window of the BRT ocean analysis and in the 7-day window of the second assimilation cycle of the NRT analysis.

The importance of the NRT ocean analysis

Figures 5(a) and 5(b) show the difference between two BRT ocean analyses 12 days apart (1 July minus 19 June) for (a) SST and (b) sea level. The differences are indicative of the errors in the initial conditions that would be present if the BRT analysis were used to initialize the monthly forecasts. Positive differences larger than 1 K occupy most of the Northern Hemisphere (boreal summer), with peak differences occurring around northern Europe, in the Mediterranean, and along the path of the Gulf Stream and Kuroshio currents. Negative differences larger than 0.5 K are apparent in large areas of the tropical and southern oceans. Especially noticeable are the large differences in the Arabian Sea, which may be the result of the onset of the monsoon at the end of June. The value of SST may in turn be of importance for the monsoon prediction.

The differences in sea level in Figure 5(b) are large scale, and are apparent all over the world. They are most pronounced in the Southern Hemisphere, around the northern edge of the Antartic Circumpolar Current (ACC). These differences are largely due to fast moving weather systems, which are stronger in the winter hemisphere. The basin-wide sea level differences everywhere else are mainly the result of the propagation of these barotropic disturbances. The barotropic disturbances will have a signature in the velocity field, but the vertical thermal structure is not affected. There are also some differences of a baroclinic nature confined to the Equatorial Indian and Pacific Ocean, which have an impact on the depth of the thermocline. For instance, the increased upwelling caused by the onset of the monsoon winds is visible in the Indian Ocean sea level, which is lower after the onset of the monsoon.

Figures 5(c) and 5(d) show the corresponding differences between the NRT and the BRT ocean analysis for 1 July 2005. The differences in both SST and SL are greatly reduced. In SST most of the differences are now located in the northern hemisphere, and are much smaller scale. The negative differences in the Mediterranean and North Eastern Atlantic have been eliminated. Only some negative differences remain in the extension of the Gulf Stream and the Kuroshio currents. In the tropical and southern oceans, differences in SST rarely exceed 0.5 K. The differences in sea level have almost disappeared and there are no longer basin-wide. Only some differences remain in the area around the edge of the ACC, but they are much smaller than those shown in Figure 5(b).

The importance of ocean initial conditions for extended range forecasts

Forecasts for the extended range (monthly and seasonal time scales) are made with coupled ocean-atmosphere models. These forecasts require information about the state of the ocean as well as that of the atmosphere. The relative importance of oceanic versus atmospheric initial conditions increases with the forecast range. As the atmosphere behaves in a chaotic manner beyond timescales of days, it is mainly the ocean initial conditions that carry the potential for seasonal predictability. For the monthly range, atmospheric, soil and ocean initial conditions are possibly all important.

For the monthly forecasts, initialization of the upper 100 m of the ocean may be sufficient in many places. For seasonal forecasts the ocean needs to be initialized deeper (~300–400 m) since the potential for predictability at seasonal range is thought to lie in the waters around and above the ocean thermocline. Special attention is paid to the initialization of the Equatorial Pacific, where equatorially trapped Kelvin waves can travel long distances along the equator. In general, the longer the forecast range the deeper one needs to initialize the ocean. In the eventual case of multi-annual or decadal forecasts, there may be a need to initialize the deep ocean. The predictability at multi-annual time scales is being assessed within the European projects ENSEMBLES and ENACT. On the other side of the spectrum, the short- and medium-range weather forecasts do not currently use any information from the ocean analysis (they use persisted SST). In the future they may also benefit from having an active ocean, as rapid changes of the SST associated with tropical cyclones and storm tracks may be important. The initialization of so many different time scales poses a problem for the ocean analysis system. The current set up of BRT and NRT analysis streams has potential for tailoring the assimilation parameters to allow the initialization of different time and spatial scales in the different analysis streams. However, for the time being we are using the same analysis system for monthly and seasonal forecasts (except for the operational schedule).

Numerous examples exist that illustrate the importance of the ocean initial conditions for seasonal forecasts, especially in the prediction of an El Niño event. Here we have chosen instead to present an example from the monthly forecast. Figure 6(a) shows a time-longitude section along the equator depicting the evolution of the sea level anomalies from the NRT ocean analysis, followed by the prediction from the monthly forecasting system (ensemble mean). The analysis and forecast anomalies are referred to the climatology of the analysis and coupled model respectively. For comparison the

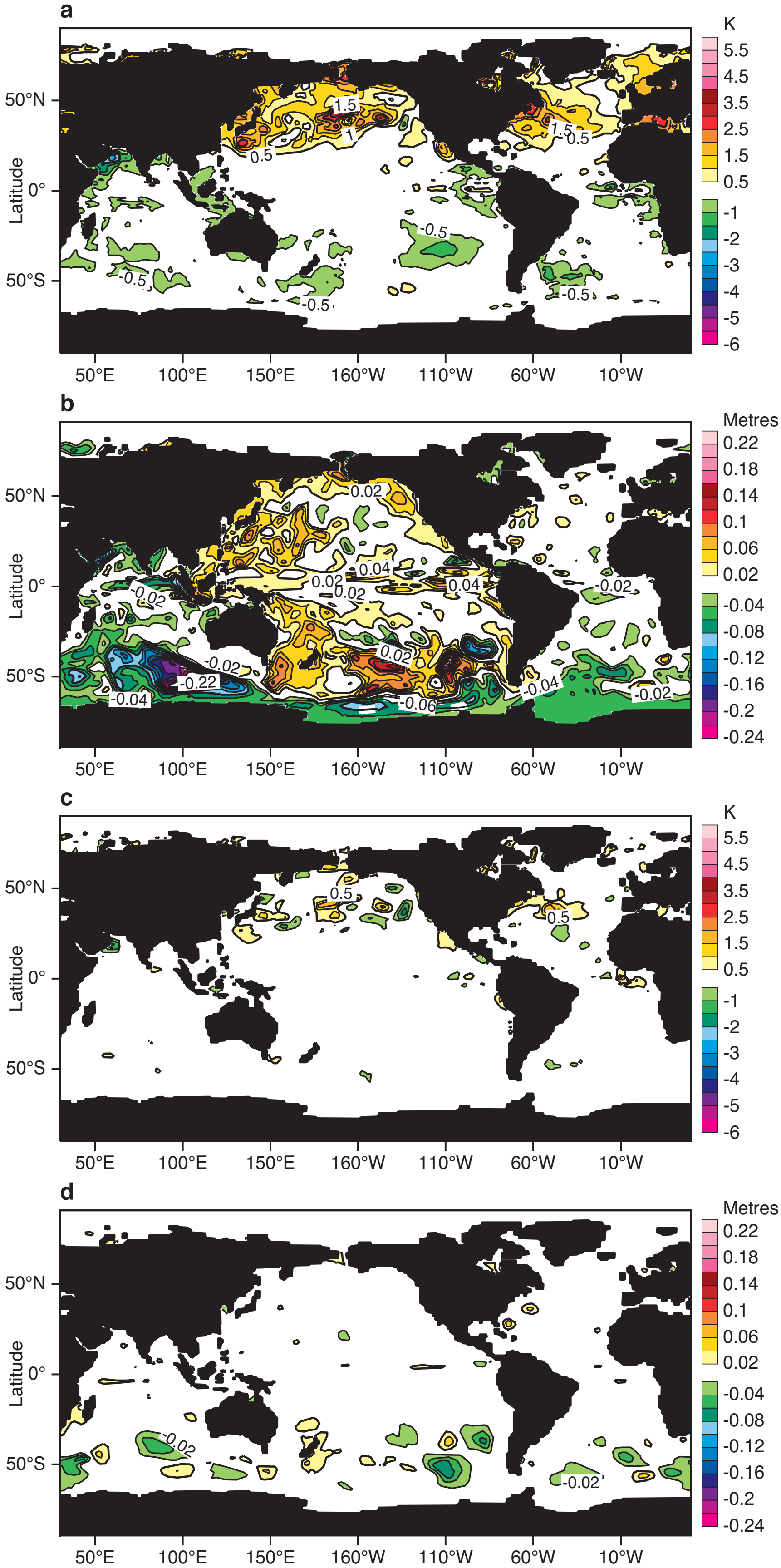

Figure 5 Differences between two BRT ocean analysis 12 days apart (1 July minus 19 June) in (a) SST (K) and (b) sea level (metres). The corresponding differences between the BRT and the NRT ocean analysis for 1 July are shown in (c) and (d).

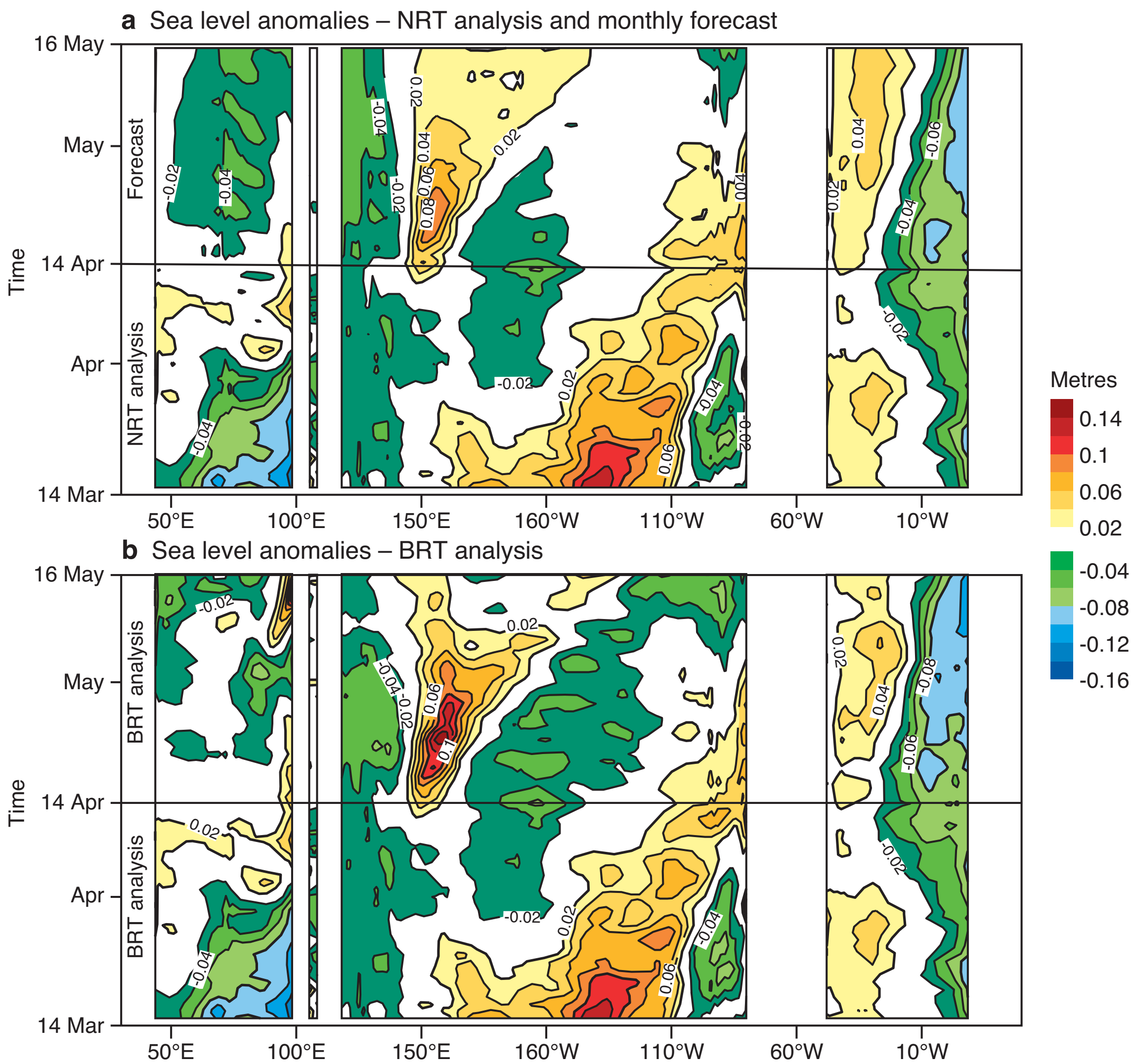

Figure 6 Time evolution of the sea level anomalies (metres) along the equator during the period 14 March to 16 May 2005. (a) The NRT analysis from the 14 March to 14 April, followed by the ensemble mean of the monthly forecast initiated on 14 April. (b) As (a) but using the BRT ocean analysis for the whole period.

evolution of the delayed analysis is shown in Figure 6(b). The differences between Figures 6(a) and 6(b) in the period 14 March to 14 April are the differences between the NRT and BRT analysis. These differences are small.

A positive anomaly in sea level is seen propagating in the analysis as a Kelvin wave during the month prior to the start of the forecast. The positive sea level anomaly is associated with a warm temperature anomaly in the subsurface. The warm anomaly will surface after a few days into the forecast, producing a warm anomaly in SST in the Eastern Pacific that was observed (not shown). The forecast was able to capture the rapid change in SST during the first days into the forecast (more than 2 K in 10 days), and the change of sign (from negative to positive anomalies, not shown).

The other feature visible in Figures 6(a) and 6(b) is the response of the ocean to the successful prediction of the westerly wind event in the Western Pacific, probably linked to a Madden Julian Oscillation (MJO): a warm anomaly is generated in the subsurface, that travels eastward as an equatorial Kelvin wave and can be seen in the evolution of sea level. The response in the forecast is slightly weaker than in the analysis, as can be expected from using the ensemble mean. As a consequence of the westerly wind burst, the SST at ~140°E cooled down by about 0.5 K (not shown). This cooling was well captured by the model.

Historical ocean reanalysis

ECMWF is heavily involved in ocean reanalysis. The main motivation for the ocean reanalysis at ECMWF is the provision of initial conditions for the calibration of coupled model forecasts. In these extended-range forecasts, model error becomes large and can not be ignored. One way to cope with model error is to refer the real-time forecasts to the model climatology. For example, the forecast anomalies in Figure 6 were computed with respect to the model climatology which is obtained by performing an extensive set of past integrations or hindcasts (commonly referred to as "back-integrations"). This in turn brings the need for extended ocean analysis into the past to provide ocean initial conditions for the calibrating hindcasts. In what follows we will refer to the historical ocean reanalysis as OR, as opposed to the ocean analysis used for the real-time forecasts, that will be referred as RT (real-time) ocean analysis, this latter encompassing both the BRT and NRT systems. Figure 7 shows schematically a summary of the components of the OR for System 2 (currently in operations) and of the future OR for System 3 (to be implemented later in the year).

The provision of initial conditions for the calibration of coupled model output sets strong constraints on the development of the ocean analysis system. Consistency between the OR and the RT systems is needed if the back integrations are to be used to calibrate the real-time forecasts. Major upgrades in the RT would have an impact on the real-time forecasts and the quality of the calibration. Therefore, the RT analysis is not changed unless a retrospective OR is performed and the back-integration recalculated. The expense of this exercise means the upgrades to the ocean analysis system are not gradual; rather, the upgrades are step-like: infrequent but substantial.

As the back-integrations from the OR ocean initial conditions are often used for skill assessment, the representation of the interannual and climate variability in the OR should be reliable. This is a tremendous challenge for any reanalysis system, subject to discontinuities due to the ever-changing nature of observing system. This is for instance the reason why altimeter data are not used in the current ECMWF ocean analysis system: by the time of its operational implementation back in 2001, the assimilation of altimeter data (available since 1993) was found to change the mean state of the ocean analysis, which would have implied limiting the extent of back-integrations to 1993. Since it is important that the back-integrations sample a wide range of climate situations, it was decided to leave the altimeter data aside. Assimilation of altimeter data is planned in the next ocean analysis system (System 3), since the assimilation will include a procedure for online estimation and correction of the bias, and the method to assimilate altimeter has been revised to ameliorate the impact on the mean state. Hopefully the benefits of using the altimeter data will outweigh the possible draw-backs.

As a result of the extended range forecast activities, ECMWF can offer to the climate community ocean reanalysis products of high quality that can be used in the study of climate variability. Figure 8 shows the evolution of upper 300 m ocean temperature, (T300) in three different regions: Eastern Pacific (Figure 8(a)), North Atlantic (Figure 8(b)) and Global (Figure 8(c)). The time series, which spans the period 1962–2002, is from a prototype of the next operational system. The evolution of T300 in the Eastern Equatorial Pacific is dominated by ENSO interannual variability, which is by no means periodic. ENSO variability in the Eastern Pacific has an amplitude ranging from 1 K to more than 3 K. The unprecedented amplitude of the 1997/8 El Niño can be appreciated, as well as the large 1982/3 event. These large events not only dominate the variability in the Eastern Pacific, but they also affect the three tropical oceans (not shown).

In the North Atlantic, the evolution of T300 shows an obvious warming trend of about 0.6 K from 1987 to 2002. The variability in T300 here relates well to the North Atlantic Oscillation (NAO) index: peak cold events during 1962/4, 1969/70, 1979, and 1995 all follow negative peaks of the NAO index. The evolution of the global temperature in the upper 300 m of the ocean since the late 1980s is clearly dominated by a large warming trend, to which the temperatures in the North Atlantic are a major contributor. There is some interdecadal variability, with the 1960s and 1980s being colder than the 1970s. The information contained in the ocean reanalysis can help to quantify and understand the role of the ocean in a changing climate.

Future developments

Later this year, the ocean analysis system will be upgraded together with the seasonal forecasting system (System 3). The new system will provide retrospective ocean analysis back to 1959 (the reanalysis for the current System 2 started in 1986). Two main developments have made this extension possible: the availability of quality forcing fields back to 1959 from the ERA-40 atmospheric analysis, and the existence of a comprehensive quality-controlled observational archive compiled as part of the ENACT project. Salinity and altimeter-derived sea level anomalies will now be assimilated as well as subsurface temperature. The possibility of using the geoid information provided by GRACE is currently being assessed. Major developments in the assimilation systems have been made to be able to assimilate salinity data, which involved the

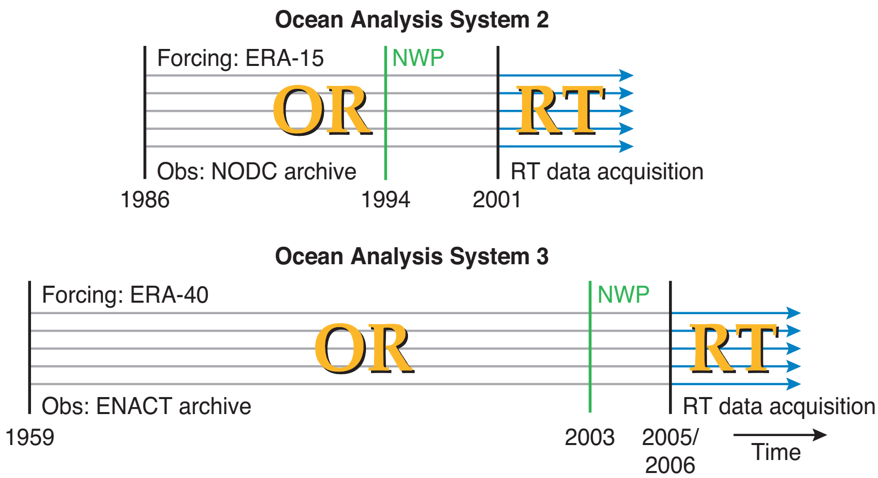

Figure 7 Schematic summary of the ocean reanalysis (OR) and real-time (RT) analysis in the current operational System 2, and planned OR and RT for System 3. The next reanalysis will use forcing fields from ERA-40 and will start in 1959. System 3 will produce an ensemble of five ocean analyses, as did System 2.

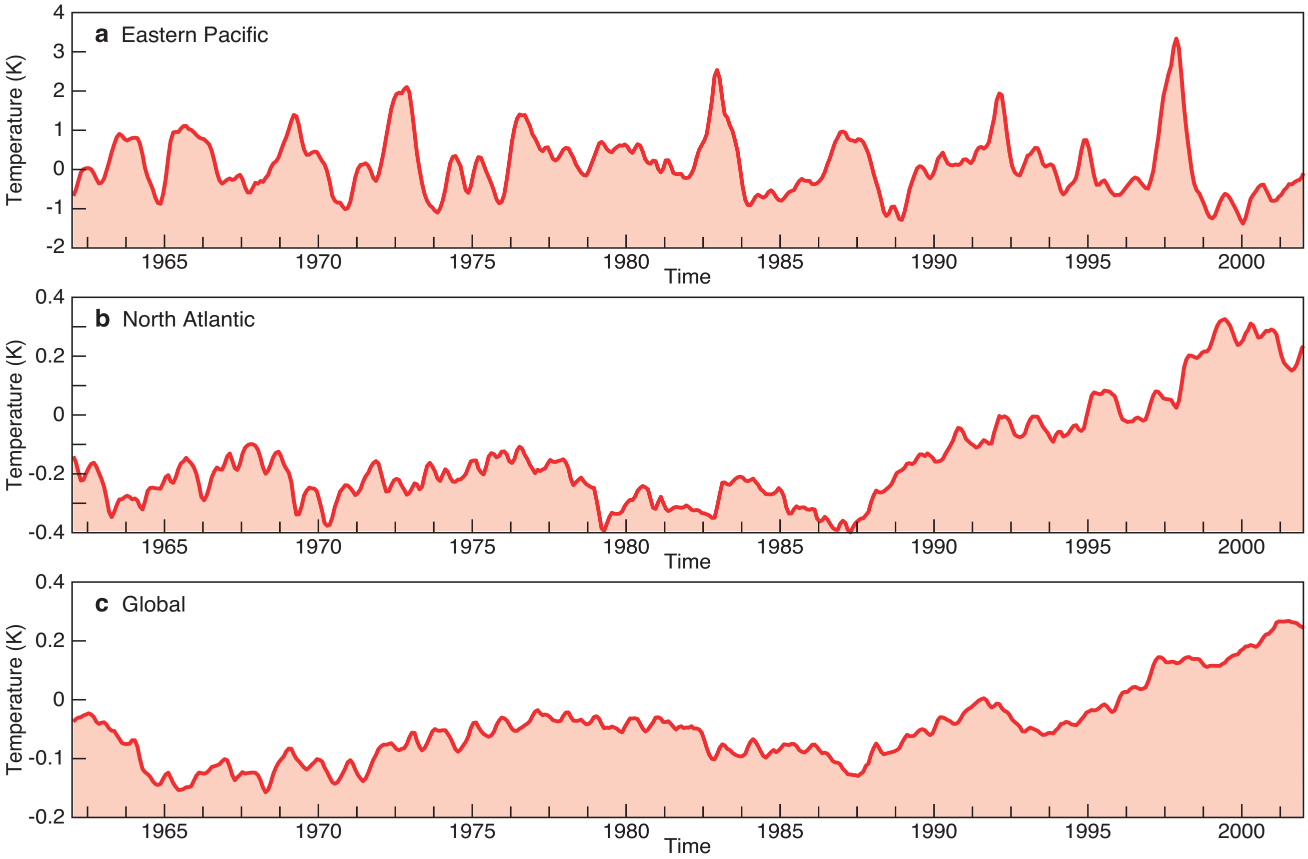

Figure 8 Time evolution of the ocean temperature averaged over the upper 300 m (T300) in three different regions: (a) Eastern Pacific, (b) North Atlantic and (c) global. ENSO variability dominates the Eastern Pacific, with the NAO impact visible in the evolution of T300 in the North Atlantic. A strong warming trend is apparent after 1987 in the global T300. The time series are from a prototype of the next operational system, and is a contribution of ECMWF to the ENACT project.

formulation of isopycnal covariances of the background error. The method to assimilate altimeter data has also undergone major revision in order to avoid discontinuities in the ocean analysis mean state. There is a multivariate scheme for online estimation and correction of the bias that aims to make the ocean analysis less vulnerable to changes in the observing system. The wind perturbations used to create the ensemble of analyses have also been revised to allow for increasing uncertainty as we go further into the past.

The ECMWF ocean products, from the historical reanalysis to the real-time products, are a valuable contribution to a wide community. The historical ocean reanalyses provide a rich data set for the study and understanding of climate variability. Climate diagnostics of the historical ocean reanalysis will provide feedback about the strengths and weaknesses of the products, setting in this way the path for future development. Real-time ocean analysis products, used to initialize coupled forecasts (monthly and seasonal), are also used to monitor the state and evolution of the global oceans. Real-time ocean analyses of the subsurface are used together with the seasonal forecasts of SST to produce the routine statements needed by the WMO ENSO advisory committee. The SST forecasts from the seasonal forecasting system can be used as boundary conditions to produce seasonal forecasts with atmosphere-only models. Finally, the monthly forecasting system produces an ensemble of global ocean forecasts every seven days. The timeliness of the monthly system can assist decision makers involved with the latest SST forecasts and ENSO related problems.

System 3 will be probably the last operational system that uses the HOPE model and the OI assimilation system. The new ocean component will use the OPA ocean model developed at the Laboratoire d'Océanographie Dynamique et de Climatologie in Paris, and the assimilation will be variational, based on the OPAVAR system developed at CERFACS in Toulouse. Changes in the horizontal and vertical resolution are also planned. In the next few years major development is need to prepare a reliable operational system based on these components. Strong collaboration with external partners will be required.

A final remark on the importance of atmospheric reanalysis: the quality of the ocean analyses is determined by the quality of the forcing fields. ERA-40 has made possible the extension of the ocean reanalysis back to 1959. For the same reason, it would be desirable that the production of atmospheric reanalyses were not conceived with a specific end date, but were kept nearly up to real time. This has the potential of improving the skill of the extended range forecasts by improving the consistency between the historical and the real-time products needed in the calibration process.

FURTHER READING

Alves O., **M. Balmaseda**, **D. Anderson** and **T. Stockdale**, 2004: Sensitivity of dynamical seasonal forecasts to ocean initial conditions. *Q. J. R. Meteorol. Soc.*, **130**, 647-668.

Balmaseda, M.A., 2004: Ocean data assimilation for seasonal forecasts. *Proceedings of ECMWF Seminar on Recent Developments in Data Assimilation for Atmosphere and Ocean*, 8-12 September 2003, 301–326.

Palmer, T.N. and **D.L.T. Anderson**, 1994: The prospects for seasonal forecasting - a review paper. *Q. J. R. Meteorol. Soc.*, **120**, 755–793.

Vialard, J., **F. Vitart**, **M.A. Balmaseda**, **T.N. Stockdale** and **D.L.T. Anderson**, 2005: An ensemble generation method for seasonal forecasting with an ocean-atmosphere coupled model. *Mon. Wea. Rev.*, **131**, 1379–1395.

ECMWF Calendar 2005/2006

2005	
Nov 8–11	Workshop – Bias Estimation and Correction in Data Assimilation (ECMWF/NWP-SAF Workshop)
Nov 14–18	Workshop – Meteorological Operational System (*10th Workshop*)
Dec 6–7	Council (*64th Session*)
2006	
Feb 6–10	GEMS Assembly
Feb 16–17	Computer Training Course – SMS/XCdp
Feb 20–24	Training Course – Introduction for new users/MARS
Feb 27–28	Computer Training Course – MAGICS
Mar 1–3	Computer Training Course – METVIEW
Mar 6–10	Computer Training Course – Use of supercomputing resources
Mar 13–17	Meteorological Training Course – Use and interpretation of ECMWF products
Mar 22–31	Meteorological Training Course – Data assimilation and use of satellite data
Apr 24–28	Meteorological Training Course – Predictability, diagnostics and seasonal forecasting
Apr 24–25	Finance Committee (*76th Session*)
Apr 25–26	Advisory Committee on Data Policy (*7th Session*)
Apr 26–27	Policy Advisory Committee (*23rd Session*)

2006	
May 2–12	Meteorological Training Course – Parametrization of diabatic processes
May 15–24	Meteorological Training Course – Numerical methods and adiabatic formulation of models
May 16–17	Security Representatives' Meeting
May 18–19	Computer Representatives Meeting
Jun 5–9	Training Course – Use and interpretation of ECMWF products
Jun 14–16	Forecast Products Users Meeting
Jul 5–6	Council (*65th Session*), Oslo
Oct 2–4	Scientific Advisory Committee (*35th Session*)
Oct 4–6	Technical Advisory Committee (*36th Session*)
Oct 9–13	Meteorological Training Course – Use and interpretation of ECMWF products for WMO Members
Oct 16–17	Finance Committee (*77th Session*)
Oct 18–19	Policy Advisory Committee (*24th Session*)
Oct 25	Advisory Committee of Co-operating States (*12th Session*)
Nov 13–17	Workshop – High performance computing in meteorology (*12th Workshop*)
Nov 27–28	Council (*66th Session*)

Dates of events coloured blue are to be confirmed.

ECMWF publications

(see www.ecmwf.int/publications/)

Technical Memoranda

474 **Matricardi, M**: The inclusion of aerosols and clouds in RTIASI, the ECMWF fast radiative transfer model for the infrared atmospheric sounding interferometer. *July 2005*

473 **Jung, T.**, **T.N. Palmer** and **G.J. Shutts**: Influence of stochastic physics on the frequency of occurrence of North Pacific weather regimes in the ECMWF model. *July 2005*

472 **Jung, T.** and **J. Barkmeijer**: Sensitivity of the tropospheric circulation to changes in the strength of the stratospheric polar vortex. *July 2005*

471 **Jung, T.**, **A.M. Tompkins** and **M.J. Rodwell**: Some aspects of systematic error in the ECMWF model. *July 2005*

470 **Jung, T.** and **F. Vitart**: Medium-range weather forecasting in the extratropics during wintertime with and without an interactive ocean. *July 2005*

469 **Tremolet, Y.**: Incremental 4D-Var convergence study. *July 2005*

467 **Radnoti, G.**, **Y. Tremolet**, **E. Andersson**, **L. Isaksen**, **E. Holm** and **M. Janisková**: Diagnostics of linear and incremental approximations in 4D-Var revisited for higher resolution analysis. *June 2005*

463 **Lalaurette, F.**, **J. Bidlot**, **L. Ferranti**, **A. Ghelli**, **F. Grazzini**, **M. Leutbecher**, **J-E. Paulsen** and **P. Viterbo**: Verification statistics and evaluations of ECMWF forecasts in 2003-2004. *May 2005*

ERA-40 Project Report Series

25 **Betts, A.K.** and **P. Viterbo**: Land-surface, boundary layer and cloud-field coupling over the south-western Amazon in ERA-40. *June 2005*

24 **Hagemann, S., K. Arpe** and **L. Bengtsson**: Validation of the hydrological cycle of ERA-40. *June 2005*

23 **Haimberger, L.**: Homogenization of radiosonde temperature time series using ERA-40 analysis feedback information. *June 2005*

ECMWF-ARM Report Series

1 **Cheinet, S., A. Beljaars, M. Kohler, J-J. Morcrette** and **P. Viterbo**: Assessing physical processes in the ECMWF model forecasts using the ARM SGP observations. *July 2005*

Workshop Proceedings

Workshop on Representation of Sub-grid Processes using Stochastic-dynamic Models. *6-8 June 2005*

Index of past newsletter articles

This is a selection of articles published in the ECMWF Newsletter series during the last five years. Articles are arranged in date order within each subject category. Articles can be accessed on the ECMWF public web site

www.ecmwf.int/publications/newsletter/index.html

	No.	Date	Page
GENERAL			
Long-term co-operation established with ESA	104	Summer 2005	3
ECMWF's highlights for 2005	103	Spring 2005	2
ECMWF and THORPEX: A natural partnership	103	Spring 2005	4
Collaboration with the Executive Body of the Convention on Long-Range Transboundary Air Pollution	103	Spring 2005	24
Co-operation Agreement with Lithuania	103	Spring 2005	24
The Centre's Building Programme	103	Spring 2005	25
25 years since the first operational forecast	102	Winter 2004/05	36
Retirement of David Burridge	101	Summer/Autumn 2004	33
ECMWF programme of activities 2003–2006	96	Winter 2002/03	36
ECMWF external policy	95	Autumn 2002	14
The Hungarian NMS	93	Spring 2002	17
COMPUTING			
Archiving, Data Provision and Visualisation			
A simple false-colour scheme for the representation of multi-layer clouds	101	Summer/Autumn 2004	30
The ECMWF public data server	99	Autumn/Winter 2003	19
A description of ECMWF's next-generation data-handling system	93	Spring 2002	15
MARS on the Web: a virtual tour	90	Spring 2001	9
New physics parameters in the MARS archive	90	Spring 2001	17
Computers, Networks and Systems, and Web			
Developing and validating Grid Technology for the solution of complex meteorological problems	104	Summer 2005	22
Migration of ECFS data from TSM to HPSS ("Back-archive")	103	Spring 2005	22
New ECaccess features	98	Summer 2003	31
Migration of the high-performance computing service to the new IBM supercomputers	97	Spring 2003	20
ECaccess: A portal to ECMWF	96	Winter 2002/03	28
ECMWF's new web site	94	Summer 2002	11

	No.	Date	Page
Computers, Networks and Systems, and Web			
The new High-Performance Computing Facility (HPCF)	93	Spring 2002	11
Linux experience at ECMWF	92	Autumn 2001	12
The RMDCN Project in RA VI	89	Winter 2000/01	12
Programming			
Programming for the IBM high-performance computing facility	94	Summer 2002	9
IFS tests using MPI/OpenMP	88	Summer/Autumn 2000	13
METEOROLOGY			
Observations and Assimilation			
CO_2 from space: estimating atmospheric CO_2 within the ECMWF data assimilation system	104	Summer 2005	14
Sea ice analyses for the Baltic Sea	103	Spring 2005	6
The ADM-Aeolus satellite to measure wind profiles from space	103	Spring 2005	11
An atlas describing the ERA-40 climate during 1979–2001	103	Spring 2005	20
Planning of adaptive observations during the Atlantic THORPEX Regional Campaign 2003	102	Winter 2004/05	16
ERA-40: ECMWF's 45-year reanalysis of the global atmosphere and surface conditions 1957-2002	101	Summer/Autumn 2004	2
Assimilation of high-resolution satellite data	97	Spring 2003	6
Assimilation of meteorological data for commercial aircraft	95	Autumn 2002	9
Ensemble Prediction			
EPS skill improvements between 1994 and 2005	104	Summer 2005	10
Ensembles-based predictions of climate change and their impacts (ENSEMBLES Project)	103	Spring 2005	16
Operational limited-area ensemble forecasts based on 'Lokal Modell'	98	Summer 2003	2
Ensemble forecasts: can they provide useful early warnings?	96	Winter 2002/03	10
Trends in ensemble performance	94	Summer 2002	2
Weather risk management with the ECMWF Ensemble Prediction System	92	Autumn 2001	7

Ensemble prediction

	No.	Date	Page
The new 80-km high-resolution ECMWF EPS	90	Spring 2001	2
The future of ensemble prediction	88	Summer/Autumn 2000	2

Environmental monitoring

	No.	Date	Page
A preliminary survey of ERA-40 users developing applications of relevance to GEO (Group on Earth Observations)	104	Summer 2005	5
The GEMS project – making a contribution to the environmental monitoring mission of ECMWF	103	Spring 2005	17
Environmental activities at ECMWF	99	Autumn/Winter 2003	18

Forecast model

	No.	Date	Page
Improved prediction of boundary layer clouds	104	Summer 2005	18
Two new cycles of the IFS: 26r3 and 28r1	102	Winter 2004/05	15
Early delivery suite	101	Summer/Autumn 2004	21
Systematic errors in the ECMWF forecasting system	100	Spring 2004	14
A major new cycle of the IFS: Cycle 25r4	97	Spring 2003	12
Verification of precipitation forecasts using data from high-resolution observation networks	93	Spring 2002	2
Impact of the radiation transfer scheme RRTM	91	Summer 2001	2
Revised land-surface analysis scheme in the IFS	88	Summer/Autumn 2000	8

Meteorological applications

	No.	Date	Page
Early medium-range forecasts of tropical cyclones	102	Winter 2004/05	7
European Flood Alert System	101	Summer/Autumn 2004	30
Model predictions of the floods in the Czech Republic during August 2002: The forecaster's perspective	97	Spring 2003	2
Joining the ECMWF improves the quality of forecasts	94	Summer 2002	6
Forecasts for the Karakoram mountains	92	Autumn 2001	3

Meteorological studies

	No.	Date	Page
Starting-up medium-range forecasting for New Caledonia in the South-West Pacific Ocean – a not so boring tropical climate	102	Winter 2004/05	2
A snowstorm in North-Western Turkey 12–13 February 2004 – Forecasts, public warnings and lessons learned	102	Winter 2004/05	7
The exceptional warm anomalies of summer 2003	99	Autumn/Winter 2003	2
Record-breaking warm sea surface temperatures of the Mediterranean Sea	98	Summer 2003	30
Breakdown of the stratospheric winter polar vortex	96	Winter 2002/03	2
Central European floods during summer 2002	96	Winter 2002/03	18
Dreaming of a white Christmas!	93	Spring 2002	8
Severe weather prediction using the ECMWF EPS: the European storms of December 1999	89	Winter 2000/01	2

Ocean and wave modelling

	No.	Date	Page
MERSEA – a project to develop ocean and marine applications	103	Spring 2005	21
Towards freak-wave prediction over the global oceans	100	Spring 2004	24
Probabilistic forecasts for ocean waves	95	Autumn 2002	2
ECMWF wave-model products	91	Summer 2001	9

Monthly and seasonal forecasting

	No.	Date	Page
Monthly forecasting	100	Spring 2004	3
DEMETER: Development of a European multi-model ensemble system for seasonal to interannual prediction	99	Autumn/Winter 2003	8
The ECMWF seasonal forecasting system	98	Summer 2003	17
Did the ECMWF seasonal forecasting model outperform a statistical model over the last 15 years?	98	Summer 2003	26

Useful names and telephone numbers within ECMWF

Telephone

Telephone number of an individual at the Centre is:

International: +44 118 949 9 + three digit extension
UK: (0118) 949 9 + three digit extension
Internal: 2 + three digit extension

e.g. the Director's number is:
+44 118 949 9001 (international),
(0118) 949 9001 (UK) and 2001 (internal).

E-mail

The e-mail address of an individual at the Centre is:
firstinitial.lastname@ecmwf.int

e.g. the Director's address is: D.Marbouty@ecmwf.int

For double-barrelled names use a hyphen
e.g. J-N.Name-Name@ecmwf.int

Internet web site

ECMWF's public web site is: http://www.ecmwf.int

	Ext
Director	
Dominique Marbouty	001
Deputy Director & Head of Administration Department	
Gerd Schultes	007
Head of Operations Department	
Walter Zwieflhofer	003
Head of Research Department	
Philippe Bougeault	005

Switchboard

ECMWF switchboard	000

Advisory

Internet mail addressed to Advisory@ecmwf.int
Telefax (+44 118 986 9450, marked User Support)

Computer Division

Division Head	
Isabella Weger	050
Computer Operations Section Head	
Sylvia Baylis	301
Networking and Computer Security Section Head	
Matteo Dell'Acqua	356
Servers and Desktops Section Head	
Richard Fisker	355
Systems Software Section Head	
Neil Storer	353
User Support Section Head	
Umberto Modigliani	382
User Support Staff	
John Greenaway	385
Paul Dando	381
Dominique Lucas	386
Carsten Maaß	389
Pam Prior	384

Computer Operations

Call Desk	303
Call Desk email: cdk@ecmwf.int	
Console – Shift Leaders	803
Console fax number +44 118 949 9840	
Console email: newops@ecmwf.int	
Fault reporting – Call Desk	303
Registration – Call Desk	303
Service queries – Call Desk	303
Tape Requests – Tape Librarian	315

Software libraries (eclib, nag, etc.)

John Greenaway	385

Meteorological Division

	Ext
Division Head	
Horst Böttger	060
Meteorological Applications Section Head	
Alfred Hofstadler	400
Data and Services Section Head	
Baudouin Raoult	404
Graphics Section Head	
Jens Daabeck	375
Meteorological Operations Section Head	
David Richardson	420
Meteorological Analysts	
Antonio Garcia Mendez	424
Federico Grazzini	421
Anna Ghelli	425
Claude Gibert (web products)	111
Laura Ferranti (seasonal forecasts)	601
Meteorological Operations Room	426

Data Division

Division Head	
Adrian Simmons	700
Data Assimilation Section Head	
Erik Andersson	627
Satellite Data Section Head	
Jean-Nöel Thépaut	621
Re-Analysis Project (ERA) Head	
Saki Uppala	366

Probabilistic Forecasting & Diagnostics Division

Division Head	
Tim Palmer	600
Seasonal Forecasting Section Head	
David Anderson	706

Model Division

Division Head	
Martin Miller	070
Numerical Aspects Section Head	
Mariano Hortal	147
Physical Aspects Section Head	
Anton Beljaars	035
Ocean Waves Section Head	
Peter Janssen	116

GMES Coordinator

Anthony Hollingsworth	824

Education & Training

Renate Hagedorn	257

ECMWF library & documentation distribution

Els Kooij-Connally	751